LEARNING BACKPROPAGATION-FREE DEEP ARCHITECTURES WITH KERNELS

Anonymous authors
Paper under double-blind review

ABSTRACT

One can substitute each neuron in any neural network with a kernel machine and obtain a counterpart powered by kernel machines. The new network inherits the expressive power and architecture of the original but works in a more intuitive way since each node enjoys the simple interpretation as a hyperplane (in a reproducing kernel Hilbert space). Further, using the kernel multilayer perceptron as an example, we prove that in classification and under certain losses, an optimal representation that minimizes the risk of the network can be characterized for each hidden layer. This result removes the need of backpropagation in learning the model and can be generalized to any feedforward kernel network. Moreover, unlike backpropagation, which turns models into black boxes, the optimal hidden representation enjoys an intuitive geometric interpretation, making the dynamics of learning in a deep kernel network transparent. Empirical results are provided to complement our theory.

1 INTRODUCTION

Any neural network (NN) can be turned into a kernel network (KN) by replacing each artificial neuron (McCulloch & Pitts, 1943), i.e., learning machine of the form $f(x) = \sigma(w^\top x + b)$, with a kernel machine, i.e., learning machine of the form $f(x) = \langle w, \phi(x) \rangle + b$ with kernel function $k(x, y) = \langle \phi(x), \phi(y) \rangle$. This combination of connectionism and kernel method enables the learning of hierarchical, distributed representations with kernels.

In terms of training, similar to NN, KN can be trained with backpropagation (BP) (Rumelhart et al., 1986). In the context of supervised learning, the need for BP in learning a deep architecture is caused by the fact that there is no explicit target information to tune the hidden layers (Rumelhart et al., 1986). Moreover, BP is usually computationally intensive and can suffer from vanishing gradient. And most importantly, BP results in hidden representations that are notoriously difficult to interpret or assess, turning deep architectures into "black boxes".

The main theoretical contribution of this paper is the following: Employing the simplest feedforward, fully-connected KN as an example, we prove that in classification and under certain losses, the optimal representation for each hidden layer that minimizes the risk of the network can be explicitly characterized. This result removes the need for BP and makes it possible to train the network in a feedforward, layer-wise fashion. And the same idea can be generalized to other feedforward KNs.

The layer-wise learning algorithm gives the same optimality guarantee as BP in the sense that it minimizes the risk. But the former is much faster and evidently less susceptible to vanishing gradient. Moreover, the quality of learning in the hidden layers can be directly assessed during or after training. Most importantly, the optimal representation for each hidden layer enjoys an intuitive geometric interpretation, making the learning dynamics in a deep KN more transparent than that in a deep NN.

To further reduce computational complexity, we show that the optimal hidden representations have a "sparse" nature, which makes possible a natural approach to speed up the upper layers of a KN without performance loss, making it a very computationally efficient model in practice.

Empirical results of feedforward, fully-connected KNs trained with the layer-wise algorithm are provided to validate the competence of the models and the effectiveness of the learning method, in which we show that the KNs compare favorably with their NN equivalents trained with BP as well as other popular deep architectures trained with BP together with unsupervised greedy pre-training.

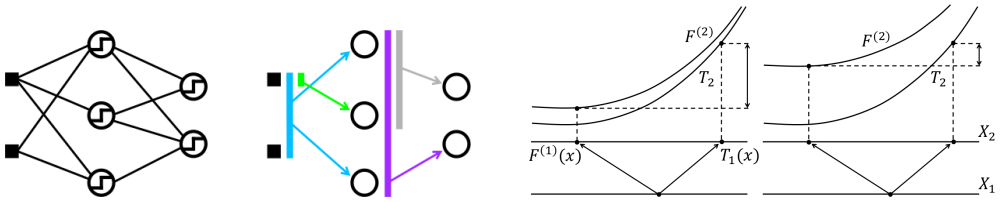

(a) (b)

Figure 1: (a) Any NN (left, presented in the usual weight-nonlinearity abstraction) can be abstracted as a "graph" (right) with each node representing a neuron and each edge the input-output relationship between neurons. If a node receives multiple inputs, we view its input as a vector in some Euclidean space, as indicated by the colored rectangles. Under this abstraction, each neuron ($f(x) = \sigma(w^\top x + b)$) can be directly replaced by a kernel machine ($f(x) = \langle w, \phi(x)\rangle + b$ with kernel $k(x, y) = \langle \phi(x), \phi(y)\rangle$) mapping from the same Euclidean space into the real line without altering the architecture and functionality of the model.
(b) Illustration for layer-wise optimality drifting away from network-optimality. Consider a two-layer network and let T_1, T_2 be the target function of the first and second layer, respectively. If the first layer creates error, which is illustrated by $F^{(1)}(x)$ being far away from $T_1(x)$, the composed solution $F^{(2)} \circ F^{(1)}$ on the right is better than that on the left and hence corresponds to the network-wise optimality. But the $F^{(2)}$ on the left is clearly a better estimate to the layer-wise optimality T_2 if the quality of estimation is measured by the supremum distance.

2 From Neural to Kernel Networks

In this section, we discuss how to build a KN using a given NN. First, the generic approach is described in Fig. 1a. Note that KN inherits the expressive power of the original NN since a kernel machine is a universal function approximator under mild conditions (Park & Sandberg, 1991; Micchelli et al., 2006) and the two models share the same architecture. However, KN works in a more intuitive way since each node is a simple linear model in a reproducing kernel Hilbert space (RKHS).

We now concretely define the KN equivalent of an l-layer Multilayer Perceptron (MLP), which we shall refer to as the kernel MLP (kMLP).[1] Given a random sample $(x_n, y_n)_{n=1}^N$, where $(x_n, y_n) \in X_1 \times Y \subset \mathbb{R}^{d_0} \times \mathbb{R}$, denote $(x_n)_{n=1}^N$ as S and $(y_n)_{n=1}^N$ as Y_S for convenience. For $i = 1, 2, \ldots, l$, consider kernel $k^{(i)} : X_i \times X_i \to \mathbb{R}$, $X_i \subset \mathbb{R}^{d_{i-1}}$ (for $i > 1$, d_{i-1} is determined by the width of the $i-1^{\text{th}}$ layer). $k^{(i)}(x, y) = \left\langle \phi^{(i)}(x), \phi^{(i)}(y)\right\rangle_{H_i}$, where $\phi^{(i)}$ is a mapping into RKHS H_i.

For $i \geq 1$, the ith layer in a kMLP, denoted $F^{(i)}$, is an array of d_i kernel machines: $F^{(i)} : X_i \to \mathbb{R}^{d_i}$, $F^{(i)} = (f_1^{(i)}, f_2^{(i)}, \ldots, f_{d_i}^{(i)})$, a d_i-tuple. Let $F^{(0)}$ be the identity map on $\mathbb{R}^{d_0}$, each $f_j^{(i)} : X_i \to \mathbb{R}$ is a hyperplane in H_i: $f_j^{(i)}(x) = \left\langle w_j^{(i)}, \phi^{(i)}\left(F^{(i-1)} \circ \cdots \circ F^{(0)}(x)\right)\right\rangle_{H_i} + b_j^{(i)}$, $w_j^{(i)} \in H_i, b_j^{(i)} \in \mathbb{R}$. In practice, $f_j^{(i)}(x)$ is usually implemented as $\sum_{n=1}^N \alpha_{nj}^{(i)} k^{(i)}\left(F^{(i-1)} \circ \cdots \circ F^{(0)}(x), F^{(i-1)} \circ \cdots \circ F^{(0)}(x_n)\right) + b_j^{(i)}$, where the $\alpha_{nj}^{(i)}, b_j^{(i)} \in \mathbb{R}$ are the learnable parameters.[2] The set of mappings $\{F^{(\ell)} \circ \cdots \circ F^{(1)} : \alpha_{nj}^{(i)}, b_j^{(i)} \in \mathbb{R}$ for all admissible $n, j, i\}$ defines an l-layer kMLP. In the rest of this paper, we shall restrict our discussions to this kMLP.

3 Assumptions and Notations

We now specify the assumptions that we impose on all kernels considered in this paper. First, we consider real, continuous, symmetric kernels only and we call a kernel positive semidefinite (PSD) or positive definite (PD) if for any S, the kernel matrix defined as $(G)_{mn} = k(x_m, x_n)$ is PSD or PD, respectively. We shall always assume that any kernel considered is at least PSD and that

[1] A PyTorch-based (Paszke et al., 2017) library for implementing kMLP and the proposed layer-wise learning algorithm as well as the code and data for all experiments in this paper are available at: *anonymized URL*.

[2] The optimality of this expansion will be later justified in Section 4 under the layer-wise setting using representer theorem (Schölkopf et al., 2001).

$k^{(i)}(x,x) = c < +\infty$ for all $x \in X_i$ and $\inf_{x,y \in X_i} k^{(i)}(x,y) = a > -\infty$. It is straightforward to check using Cauchy-Schwarz inequality that the first condition implies $\max_{x,y \in X_i} k^{(i)}(x,y) = c$. For each fixed $x \in X_i$, we assume that $k^{(i)}(x,y)$, as a function of y, is $L_x^{(i)}$-Lipschitz with respect to the Euclidean metric on X_i. Let $\sup_{x \in X_i} L_x^{(i)} = L^{(i)}$, which we assume to be finite.

The following notations will be used whenever convenient: We use the shorthand $F^{(1)}(S)$ for $(F^{(1)}(x_n))_{n=1}^N$. For $i = 2, 3, \ldots, l$, $F^{(i)}(S) \coloneqq F^{(i)} \circ F^{(i-1)} \circ \cdots \circ F^{(1)}(S)$. Throughout this paper, notations such as $F^{(i)}$ can either be used to denote a set of functions or a specific function in some set depending on the context. Also, when there is no confusion, we shall suppress the dependency of any loss function on the example for brevity, i.e., for a loss function ℓ, instead of writing $\ell(f(x), y)$, we shall write $\ell(f)$.

4 A Layer-wise Learning Algorithm

To simplify discussion, we shall restrict ourselves to binary classification ($Y = \{+1, -1\}$) and directly give the result on classification with more than two classes in the end. A generalization to regression is left as future work. Again, we only focus on kMLP although the idea can be directly generalized to all feedforward KNs. We now discuss the layer-wise learning algorithm, beginning by addressing the difficulties with training a deep architecture layer-by-layer.

4.1 Fundamental Difficulties

There are two fundamental difficulties with learning a deep architecture layer-wise. First, the hidden layers do not have supervision (labels) to learn from. And it depends on BP to propagate supervision from the output backward (Rumelhart et al., 1986). We shall prove that for kMLP, one can characterize the optimal target representation for each hidden layer, which induces a risk for that layer. The target is optimal in the sense that it minimizes the risk of the subsequent layer and eventually that of the network if all layers succeed in learning their optimal representations. This optimal representation defines what we call "layer-wise optimality".

The other difficulty with layer-wise learning is that for any given hidden layer, when the upstream layers create error, layer-wise optimality may not coincide with "network-wise optimality", i.e., the solution of this layer that eventually leads to the composed solution that minimizes the risk of the network in this suboptimal case. Indeed, when a hidden layer creates error, the objective of any layer after it becomes learning a solution that is a compromise between one that is close to the layer-wise optimality and one that prevents the error from the "bad" layer before it from "getting through" easily. And the best compromise is the network-wise optimality. The two solutions may not coincide, as shown in the toy example in Fig. 1b.

Clearly, we would like to always learn the network-wise optimality at each layer, but the learner is blind to it if it is only allowed to work on one layer at a time. By decomposing the overall error of the network into error at each layer, we prove that in fact, network-wise optimality is learnable for each hidden layer even in a purely layer-wise fashion and that the proposed layer-wise algorithm learns network-wise optimality at each layer.

4.2 The Optimal Hidden Representations

We now address the first difficulty in layer-wise learning. The basic idea is first described in Section 4.2.1. Then we provide technical results in Section 4.2.2 and Section 4.2.3 to fill in the details.

4.2.1 Basic Idea

Given a deep architecture $\mathbf{F} \coloneqq F^{(l)} \circ \cdots \circ F^{(1)}$ and a loss function ℓ_l defined for this network which induces a risk that we wish to minimize: $R_l = \mathbf{E}\, \ell_l(\mathbf{F})$. BP views this problem in the following way: R_l is a function of $\mathbf{F}$. The learner tries to find an $\mathbf{F}$ that minimizes R_l using the random sample S with labels Y_S according to some learning paradigm such as Empirical Risk Minimization (ERM) or Structural Risk Minimization (SRM) (Vapnik, 2000; Shalev-Shwartz & Ben-David, 2014). S is considered as fixed in the sense that it cannot be adjusted by the learner.

Alternatively, one can view R_l as a function of $F^{(l)}$ and the learner tries to find an $F^{(l)}$ minimizing R_l using random sample S_{l-1} with labels Y_S according to some learning paradigm, where $S_{l-1} := F^{(l-1)} \circ \cdots \circ F^{(1)}(S)$[3]. The advantage is that the learner has the freedom to learn both the function $F^{(l)}$ and the random sample S_{l-1}. And since S_{l-1} determines the decision of the learning paradigm, which then determines R_l, R_l is now essentially a function of both $F^{(l)}$ and S_{l-1}: $R_l = \mathbf{E}\,\ell_l(F^{(l)}, S_{l-1})$.

The key result is that independently of the actual learning of $F^{(l)}$, one can characterize the sufficient condition on S_{l-1} under which R_l, as a function of S_{l-1}, is minimized, as we shall prove. In other words, the "global minimum" of R_l w.r.t. S_{l-1} can be explicitly identified prior to any training. This gives the optimal S_{l-1}, which we denote as $S^\star_{l-1}$.

Moreover, the characterization of $S^\star_{l-1}$ gives rise to a new loss function ℓ_{l-1} and thus also a new risk R_{l-1} that is a function of $F^{(l-1)} \circ \cdots \circ F^{(1)}$. Consequently, the same reasoning would allow us to deduce $S^\star_{l-2}$ before the learner learns $F^{(l-1)}$. And this analysis can be applied to each layer, eventually leading to a greedy learning algorithm that sequentially learns $F^{(1)}, F^{(2)} \circ F^{(1)*}, \ldots, F^{(l)} \circ F^{(l-1)*} \circ \cdots \circ F^{(1)*}$, in that order, where the asterisk on the superscript indicates that the corresponding layer has been learned and frozen.

The layer-wise learning algorithm provides a framework that enjoys great flexibility. To be specific, one could stop the above analysis at any layer i, then learn layers $i+1, \ldots, l$ in a greedy fashion but still learn layers $1, \ldots, i$ together with BP. Thus, it is easy to see that BP can be brought under this framework as a special case. Nevertheless, in later text, we shall stay on the one end of the spectrum where each layer is learned individually for clarity.

We now present the formal results that give the optimal hidden representations. By the reasoning above, the analysis starts from the last hidden layer (layer $l-1$) and proceeds backward.

4.2.2 Formal Results: $S^\star_{l-1}$

To begin with, we need to approximate the true classification error R_l since it is not computable. To this end, we first review a well-known complexity measure.

Definition 4.1 (*Gaussian complexity (Bartlett & Mendelson, 2002)*)**.** *Let $\mathcal{P}$ be a probability distribution on a metric space X and suppose $x_1, \ldots, x_N$ are independent random elements distributed as $\mathcal{P}$. Let $\mathcal{F}$ be a set of functions mapping from X into $\mathbb{R}$. Define*

$$\hat{\mathcal{G}}_N(\mathcal{F}) = \mathbf{E}\left[\sup_{f\in\mathcal{F}} \left|\frac{2}{N}\sum_{n=1}^{N} g_n f(x_i)\right| \,\middle|\, x_1, \ldots, x_N\right],$$

where $g_1, \ldots, g_N$ are independent standard normal random variables. The Gaussian complexity of $\mathcal{F}$ is $\mathcal{G}_N(\mathcal{F}) = \mathbf{E}\,\hat{\mathcal{G}}_N(\mathcal{F})$

Intuitively, Gaussian complexity quantifies how well elements in a given function class can be correlated with a noise sequence of length N, i.e., the g_n (Bartlett & Mendelson, 2002). Based on this complexity measure, we have the following bound on the expected classification error.

Theorem 4.2. *(Bartlett & Mendelson, 2002) For each F mapping S into X_{l-1}, let $\mathcal{F}_{l,A} = \Big\{f : x \mapsto \Big\langle w, \phi^{(l)}\big(F(x)\big)\Big\rangle_{H_l} + b \,\Big|\, \|w\|_{H_l} \le A, b \in \mathbb{R}\Big\}$. Fix $A, \gamma > 0$, with probability at least $1-\delta$ and for any $N \in \mathbb{N}$, every function $f^{(l)}$ in $\mathcal{F}_{l,A}$ satisfies*

$$P(yf^{(l)}(x) \le 0) \le \hat{R}_l(f^{(l)}) + 2\mathcal{G}_N(\mathcal{F}_{l,A}) + \left(\frac{8}{\gamma} + 1\right)\sqrt{\frac{\log(4/\delta)}{2N}},$$

where $\hat{R}_l(f^{(l)}) = \frac{1}{N}\sum_{n=1}^{N} \max(0, 1 - y_n f^{(l)}(x_n)/\gamma)$, the empirical hinge loss.

Given the assumptions on $k^{(l)}$, for any F, we have

$$\mathcal{G}_N(\mathcal{F}_{l,A}) \le 2A\sqrt{\frac{c}{N}}.$$

[3]This is in fact a *set* of random samples as $F^{(l-1)} \circ \cdots \circ F^{(1)}$ is a *set* of functions.

Without loss of generality, we shall set hyperparameter $\gamma = 1$. We now characterize $S^\star_{l-1}$. Note that for a given $f^{(l)}$, $A = \left\|w_{f^{(l)}}\right\|_{H_l}$ is the smallest nonnegative real number such that $f^{(l)} \in \mathcal{F}_{l,A}$ and it is immediate that this gives the tightest bound in Theorem 4.2. Let $\kappa = \frac{1}{N}\sum_{n=1}^{N} \mathbf{1}_{\{y_n=+\}}$.

Lemma 4.3 (*optimal S_{l-1}*)**.** *Given a learning paradigm minimizing $\hat{R}_l(f^{(l)}) + \tau\left\|w_{f^{(l)}}\right\|_{H_l}$ using representation $S_{l-1} = F(S)$, where τ is any positive constant satisfying $\tau < \sqrt{2(c-a)}\min(\kappa, 1-\kappa)$. Denote as $S^\star_{l-1}$ any representation satisfying*

$$k^{(l)}(F(x_+), F(x_-)) = a \quad \textit{and} \quad k^{(l)}(F(x), F(x')) = c \tag{1}$$

for all pairs of x_+, x_- from distinct classes in S and all pairs of x, x' from the same class. Suppose the learning paradigm returns $f^{(l)\star}$ under this representation. Let S°_{l-1} be another representation under which the learning paradigm returns $f^{(l)\circ}$. If $f^{(l)\circ}$ achieves zero hinge loss on at least one example from each class, then for any $N \in \mathbb{N}$, $\hat{R}_l(f^{(l)\star}) + \tau\left\|w_{f^{(l)\star}}\right\|_{H_l} \leq \hat{R}_l(f^{(l)\circ}) + \tau\left\|w_{f^{(l)\circ}}\right\|_{H_l}$.

The optimal representation $S^\star_{l-1}$, characterized by Eq. 1, enjoys a straightforward geometric interpretation: Examples from distinct classes are as distant as possible in the RKHS whereas examples from the same class are as concentrated as possible (see proof (C) of Lemma 4.3 for a rigorous justification). Intuitively, it is easy to see that such a representation is the "easiest" for the classifier.

The conditions in Eq. 1 can be concisely summarized in an ideal kernel matrix $G^\star$ defined as

$$(G^\star)_{mn} = a, \text{ if } y_m \neq y_n;$$
$$(G^\star)_{mn} = c, \text{ if } y_m = y_n.$$

And to have the $l-1^{\text{th}}$ layer learn $S^\star_{l-1}$, it suffices to train it to minimize some dissimilarity measure between $G^\star$ and the kernel matrix computed from $k^{(l)}$ and $F^{(l-1)}(S)$, which we denote G_{l-1}. Empirical alignment (Cristianini et al., 2002), L^1 and L^2 distances between matrices can all serve as the dissimilarity measure. To simplify discussion, we let the dissimilarity measure be the L^1 distance

$$\ell_{l-1}(F^{(l-1)}, (x_m, y_m), (x_n, y_n)) = |(G^\star)_{mn} - (G_{l-1})_{mn}|.$$

This specifies $\hat{R}_{l-1}(F^{(l-1)})$ as the sample mean of $(\ell_{l-1}(F^{(l-1)}, (x_m, y_m), (x_n, y_n)))_{m,n=1}^N$ and R_{l-1} as the expectation of ℓ_{l-1} over $(X_1, Y)\times(X_1, Y)$. Note that due to the boundedness assumption on $k^{(l)}$, $\ell_{l-1} \leq 2\max(|c|, |a|)$.

4.2.3 Formal Results: $S^\star_{l-2}, \ldots, S^\star_1$

Similar to Section 4.2.2, we first need to approximate R_{l-1}.

Lemma 4.4. *For $j = 1, 2, \ldots, d_{l-1}$, let $f_j^{(l-1)} \in \mathcal{F}_{l-1}$, where $\mathcal{F}_{l-1}$ is a given hypothesis space. There exists an absolute constant $C > 0$ such that for any $N \in \mathbb{N}$, with probability at least $1-\delta$,*

$$R_{l-1}(F^{(l-1)}) \leq \hat{R}_{l-1}(F^{(l-1)}) + \frac{4L^{(l)}Cd_{l-1}}{\max(|c|, |a|)}\mathcal{G}_N(\mathcal{F}_{l-1}) + \sqrt{\frac{8\log(2/\delta)}{N}}.$$

We are now in a position to characterize $S^\star_{l-2}$. For the following lemma only, we further assume that $k^{(l-1)}(x, y)$, as a function of (x, y), depends only on and strictly decreases in $\|x-y\|_2$ for all $x, y \in X_{l-1}$ with $k^{(l-1)}(x, y) > a$, and that the infimum $\inf_{x,y\in X_{l-1}} k^{(l-1)}(x, y) = a$ is attained in X_{l-1} at all x, y with $\|x-y\|_2 \geq \eta$. Also assume that $\inf_{x,y\in X_{l-1};\|x-y\|_2<\eta} \left|\partial k^{(l-1)}(x, y)/\partial\|x-y\|_2\right| = \iota^{(l-1)}$ is defined and is positive.

Consider an F mapping S into X_{l-1}, let $\mathcal{F}_{l-1,A} = \left\{f : x \mapsto \left\langle w, \phi^{(l-1)}\big(F(x)\big)\right\rangle_{H_{l-1}} + b \,\middle|\, \|w\|_{H_{l-1}} \leq A, b \in \mathbb{R}\right\}$. For a given $F^{(l-1)} = \left(f_1^{(l-1)}, \ldots, f_{d_{l-1}}^{(l-1)}\right)$, it is immediate that $A = \max_j \left\|w_{f_j^{(l-1)}}\right\|_{H_{l-1}}$ is the smallest nonnegative real number such that $f_j^{(l-1)} \in \mathcal{F}_{l-1,A}$ for all j, giving the tightest bound in Lemma 4.4 (recall the bound on $\mathcal{G}_N(\mathcal{F}_{l-1,A})$ in Theorem 4.2). Let $\psi = \sum_{m,n=1}^N \mathbf{1}_{\{y_m\neq y_n\}}/N^2$.

Lemma 4.5 (*optimal* S_{l-2})**.** *Given a learning paradigm minimizing* $\hat{R}_{l-1}(F^{(l-1)}) + \tau \max_j \left\| w_{f_j^{(l-1)}} \right\|_{H_{l-1}}$ *using representation* $S_{l-2} = F(S)$*, where* τ *is any positive constant satisfying* $\tau < \sqrt{2d_{l-1}(c-a)}\psi\iota^{(l-1)}$*. Denote as* $S^{\star}_{l-2}$ *any representation satisfying*

$$k^{(l-1)}(F(x_+), F(x_-)) = a \quad \textit{and} \quad k^{(l-1)}(F(x), F(x')) = c$$

for all pairs of x_+, x_- *from distinct classes in* S *and all pairs of* x, x' *from the same class. Suppose the learning paradigm returns* $F^{(l-1)\star} = \left(f_1^{(l-1)\star}, \ldots, f_{d_{l-1}}^{(l-1)\star} \right)$ *under this representation. Let* S°_{l-2} *be another representation under which the learning paradigm returns* $F^{(l-1)\circ}$*. If* $F^{(l-1)\circ}$ *achieves zero loss on at least one pair of examples from distinct classes, then for any* $N \in \mathbb{N}$*,* $\hat{R}_{l-1}(F^{(l-1)\star}) + \tau \max_j \left\| w_{f_j^{(l-1)\star}} \right\|_{H_{l-1}} \leq \hat{R}_{l-1}(F^{(l-1)\circ}) + \tau \max_j \left\| w_{f_j^{(l-1)\circ}} \right\|_{H_{l-1}}$.

Applying this analysis to the rest of the hidden layers, it is evident that each of these layers should be trained to minimize the difference between $G^{\star}$ and its own kernel matrix. Generalizing to classification with more than two classes requires no change to the algorithm since the definition of $G^{\star}$ is agnostic to the number of classes involved in the classification task. Also note that the sufficiency of expanding the kernel machines of each layer on the training sample (see Section 2) for the learning objectives in Lemma 4.3 and Lemma 4.5 is trivially justifiable since the generalized representer theorem directly applies (Schölkopf et al., 2001).

Now since the optimal representation is consistent across layers, the dynamics of layer-wise learning in a kMLP is clear: The network maps the random sample sequentially through layers, with each layer trying to map examples from distinct classes as far as possible in the RKHS while keeping examples from the same class in a cluster as concentrated as possible. In other words, each layer learns a more separable representation of the sample. Eventually, the output layer works as a classifier on the final representation and since the representation would be "simple" after the mappings of the lower layers, the learned decision boundary would generalize better to unseen data.

4.3 Finding Network-wise Optimality via Layer-wise Learning

We now discuss how to learn the network-wise optimality for each layer by working with only one layer at a time. A rigorous description of the problem of layer-wise optimality drifting away from network-wise optimality and the search for a solution begins with the following bound on the total error of any two consecutive layers in a kMLP.

Lemma 4.6. *For any* $i = 2, \ldots, l$*, let the target function and the approximation function be* $T_i, F^{(i)*} : X_i \to \mathbb{R}^{d_i}$*, respectively. Let* $\epsilon_i = \left\| F^{(i)*} - T_i \right\|_s := \sup_{x \in X_i} \left\| F^{(i)*}(x) - T_i(x) \right\|_2$*, we have*

$$\left\| F^{(i)*} \circ F^{(i-1)*} - T_i \circ T_{i-1} \right\|_s \leq \epsilon_i + \sqrt{\epsilon_{i-1}} \sqrt{2L^{(i)} \sum_{j=1}^{d_i} \left\| w_{f_j^{(i)*}} \right\|_{H_i}^2}. \tag{2}$$

By applying the above bound sequentially from the input layer to the output, we can decompose the error of an arbitrary kMLP into the error of the layers. This result gives a formal description of the problem: The hypothesis with the minimal norm minimizes the propagated error from upstream, but evidently, this hypothesis is not necessarily close to the layer-wise optimality T_i.

Moreover, this bound also provides the insight needed for learning the network-wise optimality independently at each layer: Searching for the network-wise optimality amounts to sequentially minimizing the r.h.s. of Eq. 2 from the input layer forward. And it is easy to see that the solution that minimizes $\hat{R}_i(F^{(i)}) + \tau \max_j \left\| w_{f_j^{(i)}} \right\|_{H_i}$, where $\tau > 0$ is a hyperparameter, provides a good approximate to the minimizer of the r.h.s. of Eq. 2 if, of course, τ is chosen well. This learning problem is solvable independently at each layer and the optimality of the optimal hidden representations are still guaranteed by Lemma 4.3 and Lemma 4.5. Note that for BP, one usually also needs to heuristically tune the regularization coefficient for weights as a hyperparameter.

4.4 ACCELERATING THE UPPER LAYERS

There is a natural method to accelerate the upper layers (all but the input layer): The optimal representation $F(S)$ is sparse in the sense that $\phi(F(x_m)) = \phi(F(x_n))$ if $y_m = y_n$ and $\phi(F(x_m)) \neq \phi(F(x_n))$ if $y_m \neq y_n$ (see the proof (C) of Lemma 4.3). Since a kernel machine built on this representation of the given sample is a function in the RKHS that is contained in the span of the image of the sample, retaining only one example from each class would result in exactly the same hypothesis space because trivially, we have $\{\sum_{n=1}^{N} \alpha_n \phi(F(x_n)) | \alpha_n \in \mathbb{R}\} = \{\alpha_+ \phi(F(x_+)) + \alpha_- \phi(F(x_-)) | \alpha_+, \alpha_- \in \mathbb{R}\}$ for arbitrary x_+, x_- in S when the representation $F(S)$ is optimal. Thus, after training a given layer, depending on how close the actual kernel matrix is to the ideal one, one can (even randomly) discard a large portion of centers for kernel machines of the next layer to speed up the training of it without sacrificing performance. As we will later show in the experiments, randomly keeping a fraction of the training sample as centers for upper layers produces performance comparable to or better than that obtained with using the entire training set.

5 RELATED WORKS

The idea of combining connectionism with the classical kernel method was initiated by Cho & Saul (2009). In their work, an "arc cosine" kernel was so defined as to imitate the computations performed by a one-layer MLP. Zhuang et al. (2011) extended the idea to arbitrary kernels with a focus on MKL, using an architecture very similar to a two-layer MLP with neurons substituted by kernel machines. As a further generalization, Zhang et al. (2017) independently proposed kMLP and the KN equivalent of CNN. However, they did not extend the idea to any arbitrary NN. Scardapane et al. (2017) proposed to reparameterize each nonlinearity in an NN with a kernel expansion, resulting in a network similar to KN but is trained with BP.

There are other works aiming at building "deep" kernels using approaches that are different in spirit from those above. Wilson et al. (2016) proposed to learn the covariance matrix of a Gaussian process using an NN in order to make the kernel "adaptive". This idea also underlies the now standard approach of combining a deep NN with an SVM for classification, which was first explored by Huang & LeCun (2006) and Tang (2013). Note that such an interpretation can be given to KNs as well, as we point out in Appendix B.5. Mairal et al. (2014) proposed to learn hierarchical representations by learning mappings of kernels designed to be invariant to irrelevant variations in images.

Much works have been done to improve or substitute BP in learning a deep architecture. Most aim at improving the classical method, working as add-ons for BP. The most notable ones are perhaps the popular unsupervised greedy pre-training techniques proposed by Hinton et al. (2006) and Bengio et al. (2007). To the best of our knowledge, among the works that try to completely substitute BP, none provides a comparable optimality guarantee in theory as that given by BP. Fahlman & Lebiere (1990) pioneered the idea of greedily learn the architecture of an NN. In their work, each new node is added to maximize the correlation between its output and the residual error signal. Several authors explored the idea of approximating the error signals propagated by BP locally at each layer or each node (Bengio, 2014; Carreira-Perpinan & Wang, 2014; Lee et al., 2015; Balduzzi et al., 2015; Jaderberg et al., 2016). Kulkarni & Karande (2017) proposed to train NN layer-wise using an ideal kernel matrix that is a special case of that in our work. And no theoretical results were provided to justify its optimality for NN. Zhou & Feng (2017) proposed a BP-free deep architecture based on decision trees, but the idea is very different from our work. Raghu et al. (2017) attempted to quantify the quality of hidden representations toward learning more interpretable deep architectures, sharing a motivation similar to ours.

6 EXPERIMENTS

We first evaluate kMLP on five vision benchmarks (Larochelle et al., 2007). The data sets consist of 28×28 grayscale images. The first three are binary classifications, the fourth and fifth are variants of MNIST (LeCun et al., 2010). More details are provided in Appendix A. In these experiments, we compared kMLP with other popular deep architectures including MLP, Deep Belief Network (DBN) (Hinton & Salakhutdinov, 2006) and Stacked Autoencoder (SAE) (Vincent et al., 2010). Note that we only focused on comparing with the standard, generic architectures because kMLP, as the

Table 1: All numerical entries are test errors (%) and 95% confidence intervals (%). When two results have overlapping confidence intervals, they are considered equivalent. Best results are marked in bold. For kMLP-1^{FAST} and kMLP-2^{FAST}, we also include (in parentheses) the ratio of the training set retained as centers, i.e., the number of training examples randomly chosen as centers for the first/second hidden layer divided by the size of the entire training set.

(a) Comparing kMLPs with other popular deep architectures. All kMLPs were trained with the proposed layer-wise algorithm. Performance of kMLPs is on a par with other architectures, demonstrating the competence of the model as well as the effectiveness of the learning algorithm.

	RECTANGLES	RECTANGLES-IMAGE	CONVEX	MNIST(10K)	MNIST(10K) ROTATED
MLP-1 (SGD)	7.16± 0.23	33.20± 0.41	32.25± 0.41	4.69± 0.19	18.11± 0.34
MLP-1 (ADAM)	5.37± 0.20	28.82± 0.40	30.07± 0.40	4.71± 0.19	18.64± 0.34
MLP-2 (ADAM)	4.36± 0.18	25.69± 0.38	25.68± 0.38	4.42± 0.18	17.22± 0.33
MLP-1 (RMSPROP+BN)	5.37± 0.20	23.81± 0.37	28.60± 0.40	4.57± 0.18	18.75± 0.34
MLP-2 (RMSPROP+BN)	4.22± 0.18	23.12± 0.37	23.28± 0.37	3.57± 0.16	13.73± 0.30
DBN-1	4.71± 0.19	23.69± 0.37	19.92± 0.35	3.94± 0.17	14.69± 0.31
DBN-3	2.60± 0.14	**22.50± 0.37**	**18.63± 0.34**	3.11± 0.15	**10.30± 0.27**
SAE-3	2.41± 0.13	24.05± 0.37	**18.41± 0.34**	3.46± 0.16	**10.30± 0.27**
KMLP-1	**2.24± 0.13**	23.29± 0.37	19.15± 0.34	**3.10± 0.15**	11.09± 0.28
KMLP-2	**2.24± 0.13**	23.30± 0.37	**18.53± 0.34**	3.16± 0.15	**10.53± 0.27**
KMLP-1^{FAST}	**2.36± 0.13 (0.05)**	23.86± 0.37 (0.01)	20.34± 0.35 (0.17)	**2.95± 0.15 (0.1)**	12.61± 0.29 (0.1)
KMLP-2^{FAST}	**2.21± 0.13 (0.3/0.3)**	23.24± 0.37 (0.01/0.3)	19.32± 0.35 (0.005/0.03)	3.18± 0.15 (0.3/0.3)	10.94± 0.27 (0.1/0.7)

(b) Further testing the proposed layer-wise learning algorithm and acceleration method using the standard MNIST dataset. The greedy learning scheme and the acceleration trick consistently outperforms BP and other acceleration methods on both the single-hidden-layer and two-hidden-layer kMLPs. Greedy kMLPs also compare favorably with MLPs trained with BP boosted by popular training techniques.

MLP-1 (RMSPROP+BN)	MLP-2 (RMSPROP+BN)	MLP-1 (RMSPROP+DROPOUT)	MLP-2 (RMSPROP+DROPOUT)	KMLP-1 (BP)	KMLP-1^{RFF} (BP)	KMLP-2^{RFF} (BP)
2.05± 0.28	**1.58± 0.24**	1.77± 0.26	1.67± 0.25	3.44± 0.36	2.01± 0.28	1.92± 0.27

KMLP-1^{PARAM} (BP)	KMLP-2^{PARAM} (BP)	KMLP-1 (GREEDY)	KMLP-2 (GREEDY)	KMLP-1^{FAST} (GREEDY)	KMLP-2^{FAST} (GREEDY)
1.88± 0.27	2.45± 0.30	1.77± 0.26	**1.56± 0.24**	1.75± 0.26 (0.54)	**1.47± 0.24 (1/0.19)**

KN equivalent of MLP, does not have a specialized architecture or features designed for certain application domains. These experiments also serve as proofs of concept for the learning approach, showing that the layer-wise algorithm is competent when compared to standard BP as well as BP combined with some popular greedy pre-training techniques. In particular, the DBNs and SAEs in the experiments had all been pre-trained using standard unsupervised greedy methods (Hinton et al., 2006; Bengio et al., 2007) before they were trained with BP.

Moreover, to further test the proposed layer-wise learning algorithm and the acceleration method, we compared greedily-trained kMLPs (accelerated and not accelerated) with kMLPs trained with BP accelerated by two popular methods including using a parametric representation (for each node in a kMLP, $f(x) = k(w, x)$, w learnable) and using random Fourier features (Rahimi & Recht, 2008). These comparisons were done using the standard MNIST (LeCun et al., 2010).

The experimental setup is as follows, kMLP-1 corresponds to a one-hidden-layer kMLP with the first layer consisting of 15 to 150 kernel machines using the same Gaussian kernel ($k(x, y) = e^{-\|x-y\|^2/\sigma^2}$) and the second layer being a single or ten (depending on the number of classes) kernel machines using another Gaussian kernel. Note that the Gaussian kernel does not satisfy the condition that the infimum a is attained (see the extra assumptions before Lemma 4.5), but for practical purposes, it suffices to set the corresponding entries of the ideal kernel matrix to some small value. For all of our experiments, we set $(G^\star)_{mn} = 1$ if $y_m = y_n$ and 0 otherwise. Hyperparameters were selected using the validation set. The validation set was then used in final training only for early-stopping based on validation error. For the standard MNIST, the last 5000 training examples were held out as validation set. For other datasets, see Appendix A. We also included results from the same kMLP for which we accelerated by randomly choosing a fraction of the training set as centers for the second layer after the first had been trained (kMLP-1^{FAST}). The kMLP-2 and kMLP-2^{FAST} are the two-hidden-layer kMLPs, the second hidden layers of which contained 15 to 150 kernel machines. We used Adam (Kingma & Ba, 2014) as the optimization algorithm of the layer-wise scheme. We compared kMLP with a one/two-hidden-layer MLP (MLP-1/MLP-2), a one/three-hidden-layer DBN (DBN-1/DBN-3)

and a three-hidden-layer SAE (SAE-3). Note that the sizes of the hidden layers and the total numbers of parameters of the kMLPs were significantly smaller than those of the corresponding SAEs and DBNs in these experiments, see Appendix A for details. Apart from standard stochastic gradient descent (SGD), multiple training techniques were applied to the MLPs to boost performance. These include Adam (Kingma & Ba, 2014), RMSProp (Tieleman & Hinton, 2012), dropout (Srivastava et al., 2014) and batch normalization (BN) (Ioffe & Szegedy, 2015). $\text{kMLP}^{\text{PARAM}}$ corresponds to kMLP accelerated by using parametric representations for the nodes, and kMLP^{RFF} random Fourier features (Zhang et al., 2017).

From Table 1a, we see that the performance of kMLP is on par with some of the most popular and most mature deep architectures. Also note that the accelerated kMLPs were significantly faster than the standard ones and produced results comparable to the latter even though we only randomly retained a small portion of centers. This shows that kMLP can be of practical interest even when dealing with the massive data sets in today's machine learning. These results also validate our earlier theoretical results on the layer-wise learning algorithm, showing that it compares favorably not only with BP but also BP enhanced by unsupervised greedy pre-training. Results in Table 1b further demonstrate the effectiveness of the greedy learning scheme and the acceleration trick. Also note that compared to using the layer-wise algorithm, it is extremely time/memory-consuming to train the kMLPs with BP without any acceleration method for even mid-sized datasets such as MNIST.

Nevertheless, we argue that what makes the layer-wise approach promising is not only the numbers in the tables. Namely, this framework of learning makes deep architectures more transparent and intuitive, which can serve as a tentative step toward more transparent, easy-to-understand models with strong expressive power. Also, new design paradigms are now possible under the layer-wise framework. For example, each layer can now be "debugged" individually. Moreover, since learning becomes increasingly simple for the upper layers as the representations become more and more well-behaved, these layers are usually very easy to set up and also converge very fast during training.

REFERENCES

N. Aronszajn. Theory of reproducing kernels. *Transactions of the American mathematical society*, 68(3):337–404, 1950.

F. R. Bach, G. R. Lanckriet, and M. I. Jordan. Multiple kernel learning, conic duality, and the smo algorithm. In *Proceedings of the twenty-first international conference on Machine learning*, pp. 6. ACM, 2004.

David Balduzzi, Hastagiri Vanchinathan, and Joachim M Buhmann. Kickback cuts backprop's red-tape: Biologically plausible credit assignment in neural networks. In *AAAI*, pp. 485–491, 2015.

Peter L Bartlett and Shahar Mendelson. Rademacher and gaussian complexities: Risk bounds and structural results. *Journal of Machine Learning Research*, 3(Nov):463–482, 2002.

Y. Bengio. Learning deep architectures for ai. *Foundations and trends® in Machine Learning*, 2(1): 1–127, 2009.

Y. Bengio, P. Lamblin, D. Popovici, and H. Larochelle. Greedy layer-wise training of deep networks. In *Advances in neural information processing systems*, pp. 153–160, 2007.

Yoshua Bengio. How auto-encoders could provide credit assignment in deep networks via target propagation. *arXiv preprint arXiv:1407.7906*, 2014.

Yoshua Bengio, Aaron Courville, and Pascal Vincent. Representation learning: A review and new perspectives. *IEEE transactions on pattern analysis and machine intelligence*, 35(8):1798–1828, 2013.

Miguel Carreira-Perpinan and Weiran Wang. Distributed optimization of deeply nested systems. In *Artificial Intelligence and Statistics*, pp. 10–19, 2014.

Y. Cho and L. K. Saul. Kernel methods for deep learning. In *Advances in neural information processing systems*, pp. 342–350, 2009.

Corinna Cortes and Vladimir Vapnik. Support-vector networks. *Machine learning*, 20(3):273–297, 1995.

Nello Cristianini, John Shawe-Taylor, Andre Elisseeff, and Jaz S Kandola. On kernel-target alignment. In *Advances in neural information processing systems*, pp. 367–373, 2002.

Scott E Fahlman and Christian Lebiere. The cascade-correlation learning architecture. In *Advances in neural information processing systems*, pp. 524–532, 1990.

P. Gehler and S. Nowozin. Infinite kernel learning. 2008.

M. Gönen and E. Alpaydın. Multiple kernel learning algorithms. *Journal of machine learning research*, 12(Jul):2211–2268, 2011.

G. E. Hinton and R. R. Salakhutdinov. Reducing the dimensionality of data with neural networks. *science*, 313(5786):504–507, 2006.

G. E. Hinton, S. Osindero, and Y. W. Teh. A fast learning algorithm for deep belief nets. *Neural computation*, 18(7):1527–1554, 2006.

Geoffrey E Hinton. Distributed representations. 1984.

Fu Jie Huang and Yann LeCun. Large-scale learning with svm and convolutional for generic object categorization. In *Computer Vision and Pattern Recognition, 2006 IEEE Computer Society Conference on*, volume 1, pp. 284–291. IEEE, 2006.

Sergey Ioffe and Christian Szegedy. Batch normalization: Accelerating deep network training by reducing internal covariate shift. *arXiv preprint arXiv:1502.03167*, 2015.

Max Jaderberg, Wojciech Marian Czarnecki, Simon Osindero, Oriol Vinyals, Alex Graves, David Silver, and Koray Kavukcuoglu. Decoupled neural interfaces using synthetic gradients. *arXiv preprint arXiv:1608.05343*, 2016.

Diederik P Kingma and Jimmy Ba. Adam: A method for stochastic optimization. *arXiv preprint arXiv:1412.6980*, 2014.

M. Kloft, U. Brefeld, S. Sonnenburg, and A. Zien. Lp-norm multiple kernel learning. *Journal of Machine Learning Research*, 12(Mar):953–997, 2011.

Mandar Kulkarni and Shirish Karande. Layer-wise training of deep networks using kernel similarity. *arXiv preprint arXiv:1703.07115*, 2017.

G. R. Lanckriet, N. Cristianini, P. Bartlett, L. E. Ghaoui, and M. I. Jordan. Learning the kernel matrix with semidefinite programming. *Journal of Machine learning research*, 5(Jan):27–72, 2004.

H. Larochelle, D. Erhan, A. Courville, J. Bergstra, and Y. Bengio. An empirical evaluation of deep architectures on problems with many factors of variation. In *Proceedings of the 24th international conference on Machine learning*, pp. 473–480. ACM, 2007.

Y. LeCun, Y. Bengio, and G. Hinton. Deep learning. *Nature*, 521(7553):436–444, 2015.

Yann LeCun, Corinna Cortes, and CJ Burges. Mnist handwritten digit database. *AT&T Labs [Online]. Available: http://yann. lecun. com/exdb/mnist*, 2, 2010.

Dong-Hyun Lee, Saizheng Zhang, Asja Fischer, and Yoshua Bengio. Difference target propagation. In *Joint european conference on machine learning and knowledge discovery in databases*, pp. 498–515. Springer, 2015.

Julien Mairal, Piotr Koniusz, Zaid Harchaoui, and Cordelia Schmid. Convolutional kernel networks. In *Advances in neural information processing systems*, pp. 2627–2635, 2014.

Warren S McCulloch and Walter Pitts. A logical calculus of the ideas immanent in nervous activity. *The bulletin of mathematical biophysics*, 5(4):115–133, 1943.

C. A. Micchelli, Y. Xu, and H. Zhang. Universal kernels. *Journal of Machine Learning Research*, 7 (Dec):2651–2667, 2006.

J. Park and I. W. Sandberg. Universal approximation using radial-basis-function networks. *Neural computation*, 3(2):246–257, 1991.

Adam Paszke, Sam Gross, Soumith Chintala, and Gregory Chanan. Pytorch: Tensors and dynamic neural networks in python with strong gpu acceleration, 2017.

Gilles Pisier. *The volume of convex bodies and Banach space geometry*, volume 94. Cambridge University Press, 1999.

Maithra Raghu, Justin Gilmer, Jason Yosinski, and Jascha Sohl-Dickstein. Svcca: Singular vector canonical correlation analysis for deep learning dynamics and interpretability. In *Advances in Neural Information Processing Systems*, pp. 6076–6085, 2017.

Ali Rahimi and Benjamin Recht. Random features for large-scale kernel machines. In *Advances in neural information processing systems*, pp. 1177–1184, 2008.

D. E. Rumelhart, G. E. Hinton, and R. J. Williams. Learning representations by back-propagating errors. *Nature*, 323(6088):533–538, 1986.

Simone Scardapane, Steven Van Vaerenbergh, Simone Totaro, and Aurelio Uncini. Kafnets: kernel-based non-parametric activation functions for neural networks. *arXiv preprint arXiv:1707.04035*, 2017.

B. Schölkopf, R. Herbrich, and A. J. Smola. A generalized representer theorem. In *Computational learning theory*, pp. 416–426. Springer, 2001.

Shai Shalev-Shwartz and Shai Ben-David. *Understanding machine learning: From theory to algorithms*. Cambridge university press, 2014.

Nitish Srivastava, Geoffrey Hinton, Alex Krizhevsky, Ilya Sutskever, and Ruslan Salakhutdinov. Dropout: a simple way to prevent neural networks from overfitting. *The Journal of Machine Learning Research*, 15(1):1929–1958, 2014.

Shizhao Sun, Wei Chen, Liwei Wang, Xiaoguang Liu, and Tie-Yan Liu. On the depth of deep neural networks: A theoretical view. In *AAAI*, pp. 2066–2072, 2016.

Yichuan Tang. Deep learning using linear support vector machines. *arXiv preprint arXiv:1306.0239*, 2013.

Tijmen Tieleman and Geoffrey Hinton. Lecture 6.5-rmsprop, coursera: Neural networks for machine learning. *University of Toronto, Technical Report*, 2012.

Vladimir Vapnik. The nature of statistical learning theory. 2000.

M. Varma and B. R. Babu. More generality in efficient multiple kernel learning. In *Proceedings of the 26th Annual International Conference on Machine Learning*, pp. 1065–1072. ACM, 2009.

P. Vincent, H. Larochelle, I. Lajoie, Y. Bengio, and P. A. Manzagol. Stacked denoising autoencoders: Learning useful representations in a deep network with a local denoising criterion. *Journal of Machine Learning Research*, 11(Dec):3371–3408, 2010.

Andrew Gordon Wilson, Zhiting Hu, Ruslan Salakhutdinov, and Eric P Xing. Deep kernel learning. In *Artificial Intelligence and Statistics*, pp. 370–378, 2016.

Z. Xu, R. Jin, I. King, and M. Lyu. An extended level method for efficient multiple kernel learning. In *Advances in neural information processing systems*, pp. 1825–1832, 2009.

Shuai Zhang, Jianxin Li, Pengtao Xie, Yingchun Zhang, Minglai Shao, Haoyi Zhou, and Mengyi Yan. Stacked kernel network. *arXiv preprint arXiv:1711.09219*, 2017.

Zhi-Hua Zhou and Ji Feng. Deep forest: Towards an alternative to deep neural networks. *arXiv preprint arXiv:1702.08835*, 2017.

J. Zhuang, I. W. Tsang, and S. C. Hoi. Two-layer multiple kernel learning. In *Proceedings of the Fourteenth International Conference on Artificial Intelligence and Statistics*, pp. 909–917, 2011.

APPENDIX A EXPERIMENTAL SETUP

The first data set, known as *rectangles*, has 1000 training images, 200 validation images and 50000 test images. The learning machine is required to tell if a rectangle contained in an image has a larger width or length. The location of the rectangle is random. The border of the rectangle has pixel value 255 and pixels in the rest of an image all have value 0. The second data set, *rectangles-image*, is the same with *rectangles* except that the inside and outside of the rectangle are replaced by an image patch, respectively. *rectangles-image* has 10000 training images, 2000 validation images and 50000 test images. The third data set, *convex*, consists of images in which there are white regions (pixel value 255) on black (pixel value 0) background. The learning machine needs to distinguish if the region is convex. This data set has 6000 training images, 2000 validation images and 50000 test images. The fourth data set contains 10000 training images, 2000 validation images and 50000 test images taken from MNIST. The fifth is the same as the fourth except that the digits have been randomly rotated. Sample images from the data sets are given in Fig. 2. For actual training and testing, the pixel values were normalized to [0, 1]. For detailed descriptions of the data sets, see (Larochelle et al., 2007).

Figure 2: From left to right: example from *rectangles*, *rectangles-image*, *convex*, *mnist(10k)* and *mnist(10k) rotated*.

For the other models, hyperparameters were also selected using the validation set. For the MLPs, the sizes of the hidden layers were chosen from the interval [25, 700]; for DBN-3 and SAE-3, the sizes of the three hidden layers varied in intervals [500, 3000], [500, 4000] and [1000, 6000], respectively. DBN-1 used a much larger hidden layer than DBN-3 to obtain comparable performance. A simple calculation shows that the total numbers of parameters in the kMLPs were fewer than those in the corresponding DBNs and SAEs by orders of magnitude in all experiments. Like in the training for the kMLPs, the validation set were also reserved for early-stopping in final training. The DBNs and SAEs had been pre-trained unsupervisedly before the supervised training phase, following the algorithms described in (Hinton et al., 2006; Bengio et al., 2007). More detailed settings for these models were reported in (Larochelle et al., 2007).

APPENDIX B FURTHER ANALYSIS

In this section, we provide some further analysis on kMLP and the layer-wise learning algorithm. Namely, in Appendix B.1, we give a bound on the Gaussian complexity of an l-layer kMLP, which describes the intrinsic model complexity of kMLP. In particular, the bound describes the relationship between the depth/width of the model and the complexity of its hypothesis space, providing useful information for model selection. In Appendix B.2, we give a constructive result stating that the dissimilarity measure being optimized at each hidden layer will not increase as training proceeds from the input layer to the output. This also implies that a deeper kMLP performs at least as well as its shallower counterparts in minimizing any loss function they are trained on. In Appendix B.3, a result similar to Lemma 4.3 is provided, stating that the characterization for the optimal representation can be made much simpler if one uses a more restricted learning paradigm. In fact, in contrast to Lemma 4.3, both necessary and sufficient conditions can be determined under the more restricted setting. In Appendix B.4, we provide a standard, generic method to estimate the Lipschitz constant of a continuously differentiable kernel, as this quantity has been repeatedly used in many of our results in this paper. In Appendix B.5, we state some advantages of kMLP over classical kernel machines. In particular, empirical results are provided in Appendix B.5.1, in which a two-layer kMLP consistently outperforms the classical Support Vector Machine (SVM) (Cortes & Vapnik, 1995) as

well as several SVMs enhanced by Multiple Kernel Learning (MKL) algorithms (Bach et al., 2004; Gönen & Alpaydın, 2011).

B.1 Gaussian Complexity of kMLP

We first give a result on the Gaussian complexity of a two-layer kMLP.

Lemma B.1. *Given kernel $k : X_2 \times X_2 \to \mathbb{R}$, where $X_2 \subset \mathbb{R}^{d_1}$. Let $\mathcal{F}_2 = \{f : X_2 \to \mathbb{R}, f(x) = \sum_{\nu=1}^{m} \alpha_\nu k(x_\nu, x) + b \mid \boldsymbol{\alpha} = (\alpha_1, \ldots, \alpha_m) \in \mathbb{R}^m, \|\boldsymbol{\alpha}\|_1 \leq A, b \in \mathbb{R}\}$, where the x_ν are arbitrary examples from X_2.*

Consider $\mathcal{F}_1 = \{(f_1, \ldots, f_{d_1}) : X_1 \to X_2 \mid f_j \in \Omega\}$, where Ω is a given hypothesis space that is closed under negation, i.e., if $f \in \Omega$, then $-f \in \Omega$. Define $\mathcal{F}_2 \circ \mathcal{F}_1 = \{h : x \mapsto \sum_{\nu=1}^{m} \alpha_\nu k(F(x_\nu), F(x)) + b \mid \|\boldsymbol{\alpha}\|_1 \leq A, b \in \mathbb{R}, F \in \mathcal{F}_1\}$.

If the range of some element in Ω contains 0, we have

$$\mathcal{G}_N(\mathcal{F}_2 \circ \mathcal{F}_1) \leq ALd_1\mathcal{G}_N(\Omega).$$

The above result can be easily generalized to kMLP with an arbitrary number of layers.

Lemma B.2. *Given an l-layer kMLP, for each $f_j^{(i)}(x) = \sum_{\nu=1}^{m} \alpha_{\nu j}^{(i)} k^{(i)}(F^{(i-1)}(x_\nu), F^{(i-1)}(x)) + b$, $\boldsymbol{\alpha}_j^{(i)} := (\alpha_{1j}^{(i)}, \ldots, \alpha_{mj}^{(i)}) \in \mathbb{R}^m, b \in \mathbb{R}$, assume $\|\boldsymbol{\alpha}_j^{(i)}\|_1 \leq A_i$ and let $d_l = 1$. Denote the class of functions implemented by this kMLP as $\mathcal{F}_l$, we have*

$$\mathcal{G}_N(\mathcal{F}_l) \leq d_1 \prod_{i=2}^{l} A_i L^{(i)} d_i \mathcal{G}_N(\Omega).$$

Proof. It is trivial to check that the hypothesis space of each layer is closed under negation and that there exists a function in each of these hypothesis spaces whose range contains 0. Then the result follows from repeatedly applying Lemma B.1. □

B.2 Nonincreasing Loss Across Layers

Lemma B.3. *For $i \geq 2$, assume $k^{(i)}$ is PD and fix layers $1, 2, \ldots, i-1$ at arbitrary states $F^{(1)}, F^{(2)}, \ldots, F^{(i-1)}$. Let the loss functions ℓ_i, ℓ_{i-1} be the same up to their domains, and denote both ℓ_i and ℓ_{i-1} as ℓ. Suppose layer i is trained with a gradient-based algorithm to minimize the loss $\ell(F^{(i)})$. Denote the state of layer i after training by $F^{(i)*}$. If $d_{i-1} = d_i$, there is an initialization for $F^{(i)}$ such that*

$$\ell(F^{(i)*}) \leq \ell(F^{(i-1)}). \tag{3}$$

Calculation for this initialization is specified in the proof.

For $i = 1$, under the further assumption that $X_1 \subset \mathbb{R}^{d_0}$ and $d_0 = d_1$, Eq. 3 becomes $\ell(F^{(1)*}) \leq \ell(F^{(0)})$, where $F^{(0)}$ is the identity map on X_1.

Remark B.3.1. *For the greedily-trained kMLP, Lemma B.3 applies to the hidden layers and implicitly requires that $k^{(i+1)} = k^{(i)}$ since the loss function for layer i, when viewed as a function of $F^{(i)}$, takes the form $\ell(k^{(i+1)}(F^{(i)}))$ and can be rewritten as $\ell_{k^{(i+1)}}(F^{(i)})$. Similarly, $\ell(k^{(i)}(F^{(i-1)}))$ is $\ell_{k^{(i)}}(F^{(i-1)})$. Since Lemma B.3 assumes ℓ to be the same across layers (otherwise it does not make sense to compare between layers), this forces $\ell_{k^{(i+1)}} = \ell_{k^{(i)}}$. Then it follows that $k^{(i+1)} = k^{(i)}$.*

Further, if $k^{(i+1)}$ and $k^{(i)}$ have the property that $k(x, y) = k(\bar{x}, \bar{y})$, where $\bar{x}, \bar{y}$ denote the images of x, y under an embedding of $\mathbb{R}^p$ into $\mathbb{R}^q$ $(p \leq q)$ defined by the identity map onto a p-dimensional subspace of $\mathbb{R}^q$, then the condition $d_{i-1} = d_i$ can be relaxed to $d_{i-1} \leq d_i$.

This lemma states that for a given kMLP, when it has been trained upto and including the ith hidden layer, the $i+1^{\text{th}}$ hidden layer can be initialized in such a way that the value of its loss function will be lower than or equal to that of the ith hidden layer after training. In particular, the actual hidden representation "converges" to the optimal represetation as training proceeds across layers. On the

other hand, when comparing two kMLPs, this result implies that the deeper kMLP will not perform worse in minimizing the loss function than its shallower counterpart.

In deep learning literature, results analogous to Lemma B.3 generally state that in the hypothesis space of a NN with more layers, there exists a hypothesis that approximates the target function nontrivially better than any hypothesis in that of another shallower network (Sun et al., 2016). Such an existence result for kMLP can be easily deduced from the earlier bound on its Gaussian complexity (see Lemma B.2). However, these proofs of existence do not guarantee that such a hypothesis can always be found through learning in practice, whereas Lemma B.3 is constructive in this regard. Nevertheless, one should note that Lemma B.3 does not address the risk $R = \mathbf{E}\ell$. Instead, it serves as a handy result that guarantees fast convergence of upper layers during training in practice.

B.3 Simpler Optimal Representation under More Restricted Learning Paradigms

The following lemma states that if we are willing to settle with a more restricted learning paradigm, the necessary and sufficient condition that guarantees the optimality of a representation can be characterized and is simpler than that described in Lemma 4.3. The setup for this lemma is the same as that of Lemma 4.3 except that the assumption that the numbers of examples from the two classes are equal is not needed.

Lemma B.4. *Consider a learning paradigm that minimizes $\hat{R}_l(f^{(l)}) + \tau\mathcal{G}_N(\mathcal{F}_{l,A})$ using representation $S_{l-1} = F(S)$ under the constraint that it returns an $f^{(l)\star} \in \mathcal{F}_{l,A}$ with $\hat{R}_l(f^{(l)\star}) = 0$, where τ is any positive constant. For any $N \in \mathbb{N}$, $\hat{R}_l(f^{(l)\star}) + \tau\mathcal{G}_N(\mathcal{F}_{l,A})$ is minimized over all linearly separable representations if and only if the representation $F(S)$ satisfies*

$$k^{(l)}(F(x_+), F(x_-)) = a$$

for all pairs of x_+, x_- from distinct classes in S.

B.4 Lipschitz Constant for Continuously Differentiable Kernels

In general, for a continuously differentiable function $f : \mathbb{R} \to \mathbb{R}$ with derivative f' and any $a, b \in \mathbb{R}$, $a < b$, we have

$$|f(b) - f(a)| = \left| \int_a^b f'(x)dx \right| \leq \int_a^b |f'(x)|dx \leq \max_{a \leq x \leq b} |f'(x)|(b-a).$$

This simple result can be used to bound the Lipschitz constant of a continuously differentiable kernel. For example, for Gaussian kernel $k : X \times X \to \mathbb{R}$, $X \subset \mathbb{R}$, $k(x, y) = e^{-(x-y)^2/\sigma^2}$, we have $\partial k(x, y)/\partial y = 2(x - y)k(x, y)/\sigma^2$. Hence for each fixed $x \in X$, $k(x, y)$ is Lipschitz in y with Lipschitz constant bounded by $\sup_{y \in X} \left| 2(x - y)k(x, y)/\sigma^2 \right|$. In practice, X is always compact and can be a rather small subspace of some Euclidean space after normalization of data, hence this would provide a reasonable approximation to the Lipschitz constant of Gaussian kernel.

B.5 Comparing kMLP with Classical Kernel Machines

There are mainly two issues with classical kernel machines besides their usually high computational complexity. First, despite the fact that under mild conditions, they are capable of universal function approximation (Park & Sandberg, 1991; Micchelli et al., 2006) and that they enjoy a very solid mathematical foundation (Aronszajn, 1950), kernel machines are unable to learn multiple levels of distributed representations (Bengio et al., 2013), yet learning representations of this nature is considered to be crucial for complicated artificial intelligence (AI) tasks such as computer vision, natural language processing, etc. (Bengio, 2009; LeCun et al., 2015). Second, in practice, performance of a kernel machine is usually highly dependent on the choice of kernel since it governs the quality of the accessible hypothesis space. But few rules or good heuristics exist for this topic due to its extremely task-dependent nature. Existing solutions such as MKL (Bach et al., 2004; Gönen & Alpaydın, 2011) view the task of learning an ideal kernel for the given problem to be separate from the problem itself, necessitating either designing an ad hoc kernel or fitting an extra trainable model on a set of generic base kernels, complicating training.

kMLP learns distributed, hierarchical representations because it inherits the architecture of MLP. To be specific, first, we see easily that the hidden activation of each layer, i.e., $F^{(i)}(x) \subset \mathbb{R}^{d_i}$, is a distributed representation (Hinton, 1984; Bengio et al., 2013). Indeed, just like in an MLP, each layer of a kMLP consists of an array of identical computing units (kernel machines) that can be activated independently. Further, since each layer in a kMLP is built on top of the previous layer in exactly the same way as how the layers are composed in an MLP, the hidden representations are hierarchical (Bengio et al., 2013).

Second, kMLP naturally combines the problem of learning an ideal kernel for a given task and the problem of learning the parameters of its kernel machines to accomplish that task. To be specific, kMLP performs nonparametric kernel learning alongside learning to perform the given task. Indeed, for kMLP, to build the network one only needs generic kernels, but each layer $F^{(i)}$ can be viewed as a part of a kernel of the form $k^{(i+1)}(F^{(i)}(x), F^{(i)}(y))$. The fact that each $F^{(i)}$ is learnable makes this kernel "adaptive", mitigating to some extent any limitation of the fixed generic kernel $k^{(i+1)}$. The training of layer i makes this adaptive kernel optimal as a constituent part of layer $i+1$ for the task the network was trained for. And it is always a valid kernel if the generic kernel $k^{(i+1)}$ is. Note that this interpretation has been given in a different context by Huang & LeCun (2006) and Bengio et al. (2013), we include it here only for completeness.

B.5.1 Empirical Results

We now compare a single-hidden-layer kMLP using simple, generic kernels with SVMs enhanced by MKL algorithms that used significantly more kernels to demonstrate the ability of kMLP to automatically learn task-specific kernels out of standard ones. The standard SVM and seven other SVMs enhanced by popular MKL methods were compared (Zhuang et al., 2011), including the classical convex MKL (Lanckriet et al., 2004) with kernels learned using the extended level method proposed in (Xu et al., 2009) ($\text{MKL}^{\text{LEVEL}}$); MKL with L^p norm regularization over kernel weights (Kloft et al., 2011) (L^pMKL), for which the cutting plane algorithm with second order Taylor approximation of L^p was adopted; Generalized MKL in (Varma & Babu, 2009) (GMKL), for which the target kernel class was the Hadamard product of single Gaussian kernel defined on each dimension; Infinite Kernel Learning in (Gehler & Nowozin, 2008) (IKL) with $\text{MKL}^{\text{LEVEL}}$ as the embedded optimizer for kernel weights; 2-layer Multilayer Kernel Machine in (Cho & Saul, 2009) (MKM); 2-Layer MKL (2LMKL) and Infinite 2-Layer MKL in (Zhuang et al., 2011) ($\text{2LMKL}^{\text{INF}}$).

Eleven binary classification data sets that have been widely used in MKL literature were split evenly for training and test and were all normalized to zero mean and unit variance prior to training. 20 runs with identical settings but random weight initializations were repeated for each model. For each repetition, a new training-test split was selected randomly.

For kMLP, all results were achieved using a greedily-trained, one-hidden-layer model with the number of kernel machines ranging from 3 to 10 on the first layer for different data sets. The second layer was a single kernel machine. All kernel machines within one layer used the same Gaussian kernel, and the two kernels on the two layers differed only in kernel width σ. All hyperparameters were chosen via 5-fold cross-validation. As for the other models compared, for each data set, SVM used a Gaussian kernel. For the MKL algorithms, the base kernels contained Gaussian kernels with 10 different widths on all features and on each single feature and polynomial kernels of degree 1 to 3 on all features and on each single feature. For $\text{2LMKL}^{\text{INF}}$, one Gaussian kernel was added to the base kernels at each iteration. Each base kernel matrix was normalized to unit trace. For L^pMKL, p was selected from $\{2, 3, 4\}$. For MKM, the degree parameter was chosen from $\{0, 1, 2\}$. All hyperparameters were selected via 5-fold cross-validation. From Table 2, kMLP compares favorably with other models, which validates our claim that kMLP learns its own kernels nonparametrically hence can work well even without excessive kernel parameterization. Performance difference among models can be small for some data sets, which is expected since they are all rather small in size and not too challenging. Nevertheless, it is worth noting that only 2 Gaussian kernels were used for kMLP, whereas all other models except for SVM used significantly more kernels.

Table 2: Average test error (%) and standard deviation (%) from 20 runs. Results with overlapping 95% confidence intervals (not shown) are considered equivalent. Best results are marked in bold. The average ranks (calculated using average test error) are provided in the bottom row. When computing confidence intervals, due to the limited sizes of the data sets, we pooled the 20 random samples.

	Size/Dimension	SVM	$\text{MKL}^{\text{LEVEL}}$	L^pMKL	GMKL	IKL	MKM	2LMKL	$\text{2LMKL}^{\text{INF}}$	kMLP-1
Breast	683/10	3.2± 1.0	3.5± 0.8	3.8± 0.7	3.0± 1.0	3.5± 0.7	2.9± 1.0	3.0± 1.0	3.1± 0.7	**2.4± 0.7**
Diabetes	768/8	**23.3± 1.8**	24.2± 2.5	27.4± 2.5	33.6± 2.5	**24.0± 3.0**	24.2± 2.5	**23.4± 1.6**	**23.4± 1.9**	**23.2± 1.9**
Australian	690/14	15.4± 1.4	15.0± 1.5	15.5± 1.6	20.0± 2.3	**14.6± 1.2**	14.7± 0.9	**14.5± 1.6**	**14.3± 1.6**	**13.8± 1.7**
Iono	351/33	7.2± 2.0	8.3± 1.9	7.4± 1.4	7.3± 1.8	6.3± 1.0	8.3± 2.7	7.7± 1.5	**5.6± 0.9**	**5.0± 1.4**
Ringnorm	400/20	**1.5± 0.7**	**1.9± 0.8**	3.3± 1.0	2.5± 1.0	**1.5± 0.7**	2.3± 1.0	2.1± 0.8	**1.5± 0.8**	**1.5± 0.6**
Heart	270/13	17.9± 3.0	17.0± 2.9	23.3± 3.8	23.0± 3.6	**16.7± 2.1**	17.6± 2.5	**16.9± 2.5**	**16.4± 2.1**	**15.5± 2.7**
Thyroid	140/5	6.1± 2.9	7.1± 2.9	6.9± 2.2	5.4± 2.1	5.2± 2.0	7.4± 3.0	6.6± 3.1	5.2± 2.2	**3.8± 2.1**
Liver	345/6	**29.5± 4.1**	37.7± 4.5	30.6± 2.9	36.4± 2.6	40.0± 2.9	**29.9± 3.6**	34.0± 3.4	37.3± 3.1	**28.9± 2.9**
German	1000/24	**24.8± 1.9**	28.6± 2.8	25.7± 1.4	29.6± 1.6	30.0± 1.5	**24.3± 2.3**	25.2± 1.8	25.8± 2.0	**24.0± 1.8**
Waveform	400/21	11.0± 1.8	11.8± 1.6	11.1± 2.0	11.8± 1.8	**10.3± 2.3**	**10.0± 1.6**	11.3± 1.9	**9.6± 1.6**	**10.3± 1.9**
Banana	400/2	**10.3± 1.5**	**9.8± 2.0**	12.5± 2.6	16.6± 2.7	**9.8± 1.8**	19.5± 5.3	13.2± 2.1	**9.8± 1.6**	11.5± 1.9
Rank	-	4.2	6.3	7.0	6.9	4.3	5.4	5.0	2.8	1.6

APPENDIX C PROOFS

Proof of Lemma 4.3. Throughout this proof we shall drop the layer index l for brevity. Given that the representation satisfies Eq. 1, the idea is to first collect enough information about the returned $f^\star = (w^\star, b^\star)$ such that we can compute $\hat{R}(f^\star) + \tau\|w^\star\|_H$ and then show that for any other $F'(S)$ satisfying the condition in the lemma, suppose the learning paradigm returns $f' = (w', b') \in \mathcal{F}_{A'}$, then $\hat{R}(f') + \tau\|w'\|_H \geq \hat{R}(f^\star) + \tau\|w^\star\|_H$. We now start the formal proof.

First, note that in the optimal representation, i.e., an $F(S)$ such that Eq. 1 holds, it is easy to see that $\|\phi(F(x_-)) - \phi(F(x_+))\|_H$ is maximized over all representations for all x_-, x_+.

Moreover, note that given the representation is optimal, we have $\phi(F(x)) = \phi(F(x'))$ if $y = y'$ and $\phi(F(x)) \neq \phi(F(x'))$ if $y \neq y'$: Indeed, by Cauchy-Schwarz inequality, for all $x, x' \in S$, $k(F(x), F(x')) = \langle \phi(F(x)), \phi(F(x'))\rangle_H \leq \|\phi(F(x))\|_H \|\phi(F(x'))\|_H$ and the equality holds if and only if $\phi(F(x)) = p\phi(F(x'))$ for some real constant p. Using the assumption on k, namely, that $\|\phi(F(x))\|_H = \sqrt{c}$ for all $F(x)$, we further conclude that the equality holds if and only if $p = 1$. And the second half of the claim follows simply from $c > a$. Thus, all examples from the $+$ and $-$ class can be viewed as one vector $\phi(F(x_+))$ and $\phi(F(x_-))$, respectively.

The returned hyperplane $f^\star$ cannot pass both $F(x_+)$ and $F(x_-)$, i.e., $f^\star(F(x_+)) = 0$ and $f^\star(F(x_-)) = 0$ cannot happen simultaneously since if so, first subtract $b^\star$, rotate while keeping $\|w^\star\|_H$ unchanged and add some suitable b' to get a new f' such that $f'(F(x_-)) < 0$ and $f'(F(x_+)) > 0$, then it is easy to see that $\hat{R}(f') + \tau\|w'\|_H < \hat{R}(f^\star) + \tau\|w^\star\|_H$. But by construction of the learning paradigm, this is not possible.

Now suppose the learning paradigm returns an $f^\star$ such that

$$\begin{aligned} y_+ f^\star(F(x_+)) + y_- f^\star(F(x_-)) &= \langle \phi(F(x_+)) - \phi(F(x_-)), w^\star\rangle_H \\ &= \|\phi(F(x_+)) - \phi(F(x_-))\|_H \|w^\star\|_H \cos\theta_{F,w^\star} =: \zeta. \end{aligned} \tag{4}$$

First note that for an arbitrary $\theta_{F,w^\star}$, ζ is less than or equal to 2 since one can always adjust $b^\star$ such that $y_+ f^\star(F(x_+)) = y_- f^\star(F(x_-))$ without changing ζ and hence having a larger ζ will not further reduce $\hat{R}(f^\star)$, which is 0 when $\zeta = 2$, but will result in a larger $\|w^\star\|_H$ according to Eq. 4. On the other hand, $\theta_{F,w^\star}$ must be 0 since this gives the largest ζ with the smallest $\|w^\star\|_H$. Indeed, if the returned $f^\star$ does not satisfy $\theta_{F,w^\star} = 0$, one could always shift, rotate while keeping $\|w^\star\|_H$ fixed and then shift the hyperplane back to produce another f' with $\theta_{F,w'} = 0$ and this f' results in a larger ζ if $\zeta < 2$ or the same ζ if $\zeta = 2$ but a smaller $\|w'\|_H$ by rescaling. Hence $\hat{R}(f') + \tau\|w'\|_H < \hat{R}(f^\star) + \tau\|w^\star\|_H$ but again, this is impossible.

Together with what we have shown earlier, we conclude that $2 \geq \zeta > 0$. Then for some $t \in \mathbb{R}$, we have

$$\hat{R}(f^\star) = \kappa \max(0, 1 - t) + (1 - \kappa)\max(0, 1 - (\zeta - t)).$$

First note that we can choose t freely while keeping $w^\star$ fixed by changing $b^\star$. If $\kappa = 1/2$, we have

$$\hat{R}(f^\star) = \begin{cases} 1 - \zeta/2, & \text{if } 1 \geq t \geq \zeta - 1 \\ \frac{1}{2}(1 + t - \zeta), & \text{if } t > 1 \\ \frac{1}{2}(1 - t), & \text{if } t < \zeta - 1. \end{cases}$$

Evidently, the last two cases both result in $\hat{R}(f^\star) > 1 - \zeta/2$ hence $f^\star$ must produce a t in $[\zeta - 1, 1]$ and $\hat{R}(f^\star) = 1 - \zeta/2$.

Now, when $\kappa \neq 1/2$, first observe that if $1 \geq t \geq \zeta - 1$,

$$\begin{aligned} \hat{R}(f^\star) &= \kappa(1 - t) + (1 - \kappa)(t - (\zeta - 1)) \\ &= (1 - 2\kappa)t + \kappa - (1 - \kappa)(\zeta - 1). \end{aligned}$$

If $\kappa > 1/2$, $\hat{R}(f^\star)$ decreases in t hence t must be 1 for $f^\star$, which implies $\hat{R}(f^\star) = (1 - \kappa)(2 - \zeta)$. Similarly, if $\kappa < 1/2$, $t = \zeta - 1$ and hence $\hat{R}(f^\star) = \kappa(2 - \zeta)$.

Now suppose $t \geq 1$, $\hat{R}(f^\star) = (1 - \kappa)(1 + t - \zeta)$, which increases in t and hence $t = 1$ and $\hat{R}(f^\star) = (1 - \kappa)(2 - \zeta)$. If $\kappa < 1/2$, since $(1 - \kappa)(2 - \zeta) > \kappa(2 - \zeta)$, this combination of κ and t contradicts the optimality assumption of $f^\star$.

If $t \leq \zeta - 1$, $\hat{R}(f^\star) = \kappa(1 - t) = \kappa(2 - \zeta)$, where the second equality is because $\hat{R}(f^\star)$ decreases in t. Again, $\kappa > 1/2$ leads to a contradiction.

Combining all cases, we have

$$\begin{aligned} \hat{R}(f^\star) + \tau\|w^\star\|_H &= \min(\kappa, 1 - \kappa)(2 - \zeta) + \frac{\tau\zeta}{\|\phi(F(x_+)) - \phi(F(x_-))\|_H} \\ &= \min(\kappa, 1 - \kappa)(2 - \zeta) + \frac{\tau\zeta}{\sqrt{2(c - a)}} \\ &= 2\min(\kappa, 1 - \kappa) + \left(\frac{\tau}{\sqrt{2(c - a)}} - \min(\kappa, 1 - \kappa)\right)\zeta, \end{aligned}$$

which, by the assumption on τ, strictly decreases in ζ over $(0, 2]$. Hence the returned $f^\star$ must satisfy $\zeta = 2$, which implies $\hat{R}(f^\star) = 0$ and we have

$$\hat{R}(f^\star) + \tau\|w^\star\|_H = \frac{\sqrt{2}\tau}{\sqrt{c - a}}.$$

Now, for any other $F'(S)$, suppose the learning paradigm returns f'. Let $x_+^{w'}, x_-^{w'}$ be the pair of examples with the largest $f'(F'(x_+)) - f'(F'(x_-))$. We have

$$y_+^{w'} f'(F'(x_+^{w'})) + y_-^{w'} f'(F'(x_-^{w'})) = \|\phi(F'(x_+^{w'})) - \phi(F'(x_-^{w'}))\|_H \|w'\|_H \cos\theta_{F',w'} =: \zeta'.$$

Then

$$\begin{aligned} \hat{R}(f') + \tau\|w'\|_H &\geq \tau\|w'\|_H \\ &= \frac{\tau\zeta'}{\|\phi(F'(x_+^{w'})) - \phi(F'(x_-^{w'}))\|_H \cos\theta_{F',w'}} \\ &\geq \frac{\tau|\zeta'|}{\|\phi(F'(x_+^{w'})) - \phi(F'(x_-^{w'}))\|_H} \\ &\geq \frac{2\tau}{\sqrt{2(c - a)}} \\ &\geq \hat{R}(f^\star) + \tau\|w^\star\|_H, \end{aligned}$$

where we have used the assumption that there exists x_-, x_+ with $y_- f'(F'(x_-)), y_+ f'(F'(x_+)) \geq 1$. This proves the desired result. □

Lemma C.1. *Suppose $f_1 \in \mathcal{F}_1, \ldots, f_d \in \mathcal{F}_d$ are elements from sets of real-valued functions defined on all of $X_1, X_2, \ldots, X_m$, where $X_j \subset \mathbb{R}^d$ for all j, $\mathcal{F} \subset \mathcal{F}_1 \times \cdots \times \mathcal{F}_d$. For $f \in \mathcal{F}$, define $\omega \circ f : X_1 \times \cdots \times X_m \times Y \to \mathbb{R}$ as $(x_1, \ldots, x_m, y) \mapsto \omega(f_1(x_1), \ldots, f_d(x_1), f_1(x_2), \ldots, f_d(x_m), y)$, where $\omega : \mathbb{R}^{md} \times Y \to \mathbb{R}^+ \cup \{0\}$ is bounded and L-Lipschitz for each $y \in Y$ with respect to the Euclidean metric on $\mathbb{R}^{md}$. Let $\omega \circ \mathcal{F} = \{\omega \circ f : f \in \mathcal{F}\}$. Denote the Gaussian complexity of $\mathcal{F}_i$ on X_j as $G_N^j(\mathcal{F}_i)$, if the $\mathcal{F}_i$ are closed under negation, i.e., for all i, if $f \in \mathcal{F}_i$, then $-f \in \mathcal{F}_i$, we have*

$$\mathcal{G}_N(\omega \circ \mathcal{F}) \leq 2L \sum_{i=1}^{d} \sum_{j=1}^{m} \mathcal{G}_N^j(\mathcal{F}_i). \tag{5}$$

In particular, for all j, if the x_n^j upon which the Gaussian complexities of the $\mathcal{F}_i$ are evaluated are sets of i.i.d. random elements with the same distribution, we have $\mathcal{G}_N^1(\mathcal{F}_i) = \cdots = \mathcal{G}_N^m(\mathcal{F}_i) \coloneqq \mathcal{G}_N(\mathcal{F}_i)$ for all i and Eq. 5 becomes

$$\mathcal{G}_N(\omega \circ \mathcal{F}) \leq 2mL \sum_{i=1}^{d} \mathcal{G}_N(\mathcal{F}_i).$$

This lemma is a generalization of a result on the Gaussian complexity of Lipschitz functions on $\mathbb{R}^k$ from (Bartlett & Mendelson, 2002). And the technique used in the following proof is also adapted from there.

Proof. For the sake of brevity, we prove the case where $m = 2$. The general case uses exactly the same technique except that the notations would be more cumbersome.

Let $\mathcal{F}$ be indexed by $\mathcal{A}$. Without loss of generality, assume $|\mathcal{A}| < \infty$. Define

$$X_\alpha = \sum_{n=1}^{N} \omega(f_{\alpha,1}(x_n), \ldots, f_{\alpha,d}(x_n'), y_n) g_n;$$
$$Y_\alpha = L \sum_{n=1}^{N} \sum_{i=1}^{d} (f_{\alpha,i}(x_n) g_{n,i} + f_{\alpha,i}(x_n') g_{N+n,i}),$$

where $\alpha \in \mathcal{A}$, the (x_n, x_n') are a sample of size N from $X_1 \times X_2$ and $g_1, \ldots, g_N, g_{1,1}, \ldots, g_{2N,d}$ are i.i.d. standard normal random variables.

Let arbitrary $\alpha, \beta \in \mathcal{A}$ be given, define $\|X_\alpha - X_\beta\|_2^2 = \mathbf{E}(X_\alpha - X_\beta)^2$, where the expectation is taken over the g_n. Define $\|Y_\alpha - Y_\beta\|_2^2$ similarly and we have

$$\begin{aligned}
\|X_\alpha - X_\beta\|_2^2 &= \sum_{n=1}^{N} \Big(\omega(f_{\alpha,1}(x_n), \ldots, f_{\alpha,d}(x_n'), y_n) - \omega(f_{\beta,1}(x_n), \ldots, f_{\beta,d}(x_n'), y_n) \Big)^2 \\
&\leq L^2 \sum_{n=1}^{N} \sum_{i=1}^{d} \Big((f_{\alpha,i}(x_n) - f_{\beta,i}(x_n))^2 + (f_{\alpha,i}(x_n') - f_{\beta,i}(x_n'))^2 \Big) \\
&= \|Y_\alpha - Y_\beta\|_2^2.
\end{aligned}$$

By Slepian's lemma (Pisier, 1999) and since the $\mathcal{F}_i$ are closed under negation,

$$\begin{aligned}
\frac{N}{2} \hat{\mathcal{G}}_N(\omega \circ \mathcal{F}) &= \mathbf{E}_{g_n} \sup_{\alpha \in \mathcal{A}} X_\alpha \\
&\leq 2\mathbf{E}_{g_{n,i}, g_{N+n,i}} \sup_{\alpha \in \mathcal{A}} Y_\alpha \\
&\leq \frac{N}{2} 2L \sum_{i=1}^{d} (\hat{G}_N^1(\mathcal{F}_i) + \hat{G}_N^2(\mathcal{F}_i)).
\end{aligned}$$

Taking the expectation of the x_n and x_n' on both sides, we have

$$\frac{N}{2} \mathcal{G}_N(\omega \circ \mathcal{F}) \leq \frac{N}{2} 2L \sum_{i=1}^{d} (G_N^1(\mathcal{F}_i) + G_N^2(\mathcal{F}_i)).$$

□

Proof of Lemma 4.4. Normalize ℓ_{l-1} to $[0,1]$ by dividing $2\max(|c|,|a|)$. Then the loss function becomes

$$\ell_{l-1}\big(F^{(l-1)},(x_m,y_m),(x_n,y_n)\big)=\frac{1}{2\max(|c|,|a|)}\Big|k^{(l)}\big(F^{(l-1)}(x_m),F^{(l-1)}(x_n)\big)-(G^\star)_{mn}\Big|.$$

For each fixed $(G^\star)_{mn}$,

$$\begin{aligned}
&\Big|\ell_{l-1}\big(F^{(l-1)},(x_m,y_m),(x_n,y_n)\big)-\ell_{l-1}\big(F^{(l-1)},(x'_m,y'_m),(x'_n,y'_n)\big)\Big|\\
&\le\frac{1}{2\max(|c|,|a|)}\Big|k^{(l)}\big(F^{(l-1)}(x_m),F^{(l-1)}(x_n)\big)-k^{(l)}\big(F^{(l-1)}(x'_m),F^{(l-1)}(x'_n)\big)\Big|\\
&\le\frac{1}{2\max(|c|,|a|)}\Big(\Big|k^{(l)}\big(F^{(l-1)}(x_m),F^{(l-1)}(x_n)\big)-k^{(l)}\big(F^{(l-1)}(x_m),F^{(l-1)}(x'_n)\big)\Big|\\
&\qquad+\Big|k^{(l)}\big(F^{(l-1)}(x_m),F^{(l-1)}(x'_n)\big)-k^{(l)}\big(F^{(l-1)}(x'_m),F^{(l-1)}(x'_n)\big)\Big|\Big)\\
&\le\frac{L^{(l)}}{2\max(|c|,|a|)}\Big(\Big\|F^{(l-1)}(x_n)-F^{(l-1)}(x'_n)\Big\|_2+\Big\|F^{(l-1)}(x_m)-F^{(l-1)}(x'_m)\Big\|_2\Big)\\
&\le\frac{L^{(l)}}{\max(|c|,|a|)}\Big\|\Big(F^{(l-1)}(x_n)-F^{(l-1)}(x'_n),F^{(l-1)}(x_m)-F^{(l-1)}(x'_m)\Big)\Big\|_2.
\end{aligned}$$

Hence ℓ_{l-1} is $L^{(l)}/\max(|c|,|a|)$-Lipschitz in $(F^{(l-1)}(x_m),F^{(l-1)}(x_n))$ with respect to the Euclidean metric on $\mathbb{R}^{2d_{l-1}}$ for each $(G^\star)_{mn}$.

The result follows from Lemma C.1 with $m=2, d=d_{l-1}$ and Corollary 15 in (Bartlett & Mendelson, 2002). □

Proof of Lemma 4.5. This proof uses essentially the same idea as that of Lemma 4.3. Due to the complete dependence of $k^{(l)}(x,y)$ on $\|x-y\|_2$, we can rewrite $k^{(l)}\Big(F^{(l-1)}(F(x_m)),F^{(l-1)}(F(x_n))\Big)$ as $h^{(l)}\Big(\big\|F^{(l-1)}(F(x_m))-F^{(l-1)}(F(x_n))\big\|_2\Big)$ for some $h^{(l)}$. Define $\mu_{mn}^{(l-1)}=\|\phi^{(l-1)}(F(x_m))-\phi^{(l-1)}(F(x_n))\|_{H_{l-1}}$, we have

$$\begin{aligned}
&\hat{R}_{l-1}(F^{(l-1)})\\
&=\frac{1}{N^2}\sum_{m,n=1}^{N}\Big|h^{(l)}\Big(\big\|F^{(l-1)}(F(x_m))-F^{(l-1)}(F(x_n))\big\|_2\Big)-(G^\star)_{mn}\Big|\\
&=\frac{1}{N^2}\sum_{m,n=1}^{N}\Big|h^{(l)}\Big(\sqrt{\sum_{j=1}^{d_{l-1}}\big(f_j^{(l-1)}(F(x_m))-f_j^{(l-1)}(F(x_n))\big)^2}\Big)-(G^\star)_{mn}\Big|\\
&=\frac{1}{N^2}\sum_{m,n=1}^{N}\Big|h^{(l)}\Big(\sqrt{\sum_{j=1}^{d_{l-1}}\big(\mu_{mn}^{(l-1)}\|w_{f_j^{(l-1)}}\|_{H_{l-1}}\cos\theta_{F,w_{f_j^{(l-1)}}}\big)^2}\Big)-(G^\star)_{mn}\Big|.
\end{aligned}$$

Given that the representation is optimal, we have

$$\begin{aligned}
&\hat{R}_{l-1}(F^{(l-1)})+\tau\max_{1\le j\le d_{l-1}}\|w_{f_j^{(l-1)}}\|_{H_{l-1}}\\
&=\frac{1}{N^2}\sum_{y_m\neq y_n}\Bigg(h^{(l)}\Big(\sqrt{\sum_{j=1}^{d_{l-1}}\big(\mu_{mn}^{(l-1)}\|w_{f_j^{(l-1)}}\|_{H_{l-1}}\cos\theta_{F,w_{f_j^{(l-1)}}}\big)^2}\Big)-a\Bigg)\\
&\quad+\tau\max_{1\le j\le d_{l-1}}\|w_{f_j^{(l-1)}}\|_{H_{l-1}}.
\end{aligned}$$

The returned $F^{(l-1)\star}$ must satisfy

$$\sqrt{\sum_{j=1}^{d_{l-1}} \left(\mu_{mn}^{(l-1)} \|w_{f_j^{(l-1)\star}}\|_{H_{l-1}} \cos\theta_{F,w_{f_j^{(l-1)\star}}}\right)^2} \leq \eta;$$
$$\|w_{f_1^{(l-1)\star}}\|_{H_{l-1}} = \cdots = \|w_{f_{d_{l-1}}^{(l-1)\star}}\|_{H_{l-1}} =: \|w^\star\|_{H_{l-1}};$$
$$\cos\theta_{F,w^\star} = 1.$$

The first observation is trivial since if otherwise, one can always reduce the largest $\|w_{f_j^{(l-1)\star}}\|_{H_{l-1}}$ to obtain equality to η, this gives the same $\hat{R}_{l-1}(F^{(l-1)\star})$ with a smaller $\tau \max_j \|w_{f_j^{(l-1)\star}}\|_{H_{l-1}}$. Note that if during shrinking the largest $\|w_{f_j^{(l-1)\star}}\|_{H_{l-1}}$, this element ceases to be the largest among all j, we shall continue the process with the new largest instead. To see the rest of the claim, note that for the largest of the $\|w_{f_j^{(l-1)\star}}\|_{H_{l-1}}$, we must have $\theta_{F,w_{f_j^{(l-1)\star}}} = 0$ since if not, one could shift and rotate the hyperplane and again obtain the same $\hat{R}_{l-1}(F^{(l-1)\star})$ with a smaller $\tau \max_j \|w_{f_j^{(l-1)\star}}\|_{H_{l-1}}$. Reducing the largest $\|w_{f_j^{(l-1)\star}}\|_{H_{l-1}}$ and increasing the second largest by scaling, one would get a smaller risk. It is immediate that the minimal risk (w.r.t. only the first and second largest $\|w_{f_j^{(l-1)\star}}\|_{H_{l-1}}$) is attained when the largest and the second largest $\|w_{f_j^{(l-1)\star}}\|_{H_{l-1}}$ are equal. Then a similar argument as before gives $\theta_{F,w_{f_j^{(l-1)\star}}} = 0$ for both of them. The rest of the claim follows via repeatedly applying this argument to all the $\|w_{f_j^{(l-1)\star}}\|_{H_{l-1}}$.

Define

$$|f^\star(F(x_+)) - f^\star(F(x_-))| = \|\phi^{(l-1)}(F(x_+)) - \phi^{(l-1)}(F(x_-))\|_{H_{l-1}} \|w^\star\|_{H_{l-1}}.$$

Then we have

$$\begin{aligned}
&\hat{R}_{l-1}(F^{(l-1)\star}) + \tau \max_{1\leq j\leq d_{l-1}} \|w_{f_j^{(l-1)\star}}\|_{H_{l-1}} \\
&= \psi\left(h^{(l)}\left(\sqrt{d_{l-1}}|f^\star(F(x_+)) - f^\star(F(x_-))|\right) - a\right) \\
&\quad + \frac{\tau|f^\star(F(x_+)) - f^\star(F(x_-))|}{\|\phi^{(l-1)}(F(x_+)) - \phi^{(l-1)}(F(x_-))\|_{H_{l-1}}} \\
&= \psi\left(h^{(l)}\left(\sqrt{d_{l-1}}|f^\star(F(x_+)) - f^\star(F(x_-))|\right) - a\right) \\
&\quad + \frac{\tau|f^\star(F(x_+)) - f^\star(F(x_-))|}{\sqrt{2(c-a)}}.
\end{aligned}$$

As we have shown, $\sqrt{d_{l-1}}|f^\star(F(x_+)) - f^\star(F(x_-))| \in [0, \eta]$. Let $\lambda = |f^\star(F(x_+)) - f^\star(F(x_-))|$ and differentiate the r.h.s. of the above equation w.r.t. λ and using the assumption on τ, we have

$$\sqrt{d_{l-1}}\psi\frac{dh^{(l)}(t)}{dt} + \frac{\tau}{\sqrt{2(c-a)}} < 0.$$

Hence the overall risk decreases in λ over $[0, \eta/\sqrt{d_{l-1}}]$, which implies that the returned $F^{(l-1)\star}$ must have $\lambda = \eta/\sqrt{d_{l-1}}$ and

$$\hat{R}_{l-1}(F^{(l-1)\star}) + \tau \max_{1\leq j\leq d_{l-1}} \|w_{f_j^{(l-1)\star}}\|_{H_{l-1}} = \frac{\tau\eta}{\sqrt{2d_{l-1}(c-a)}}.$$

Now for any other representation $S'_{l-2} = F'(S)$, suppose the learning paradigm returns $F^{(l-1)\prime}$. Assume without loss of generality that the largest $f_j^{(l-1)\prime}(F'(x_+)) - f_j^{(l-1)\prime}(F'(x_-))$ over all j, x_+ and x_- is attained at $j = 1$ and write $w' = w_{f_1^{(l-1)\prime}}$, $f' = f_1^{(l-1)\prime}$ for convenience. Let $x_+^{w'}$, $x_-^{w'}$

be the pair with the largest $f'(F'(x_+)) - f'(F'(x_-))$. Note that the assumption on F' implies that $f'(F'(x_+)) - f'(F'(x_-)) \geq \eta/\sqrt{d_{l-1}}$. Then we have

$$
\begin{aligned}
&\hat{R}_{l-1}(F^{(l-1)\prime}) + \tau \max_{1\leq j\leq d_{l-1}} \|w_{f_j^{(l-1)\prime}}\|_{H_{l-1}} \\
&\geq \tau \|w'\|_{H_{l-1}} \\
&= \frac{\tau |f'(F'(x_+)) - f'(F'(x_-))|}{\|\phi^{(l-1)}(F'(x_+)) - \phi^{(l-1)}(F'(x_-))\|_{H_{l-1}} |\cos\theta_{F',w'}|} \\
&\geq \frac{\tau\eta}{\sqrt{2d_{l-1}(c-a)}} \\
&= \hat{R}_{l-1}(F^{(l-1)\star}) + \tau \max_{1\leq j\leq d_{l-1}} \|w_{f_j^{(l-1)\star}}\|_{H_{l-1}},
\end{aligned}
$$

proving the lemma. □

Proof of Lemma 4.6. First, it is trivial that the so-defined s metric is indeed a metric. In particular, it satisfies the triangle inequality. For $i = 2, \ldots, l$,

$$
\begin{aligned}
&\left\| F^{(i)*} \circ F^{(i-1)*} - T_i \circ T_{i-1} \right\|_s \\
&\leq \left\| F^{(i)*} \circ F^{(i-1)*} - F^{(i)*} \circ T_{i-1} \right\|_s + \left\| F^{(i)*} \circ T_{i-1} - T_i \circ T_{i-1} \right\|_s \\
&\leq \sup_{x\in X_i} \sqrt{\sum_{j=1}^{d_i} \left(f_j^{(i)*} \circ F^{(i-1)*}(x) - f_j^{(i)*} \circ T_{i-1}(x) \right)^2} + \epsilon_i \\
&= \sup_{x\in X_i} \sqrt{\sum_{j=1}^{d_i} \left(\left\langle f_j^{(i)*}(\lambda), k^{(i)}(\lambda, F^{(i-1)*}(x)) - k^{(i)}(\lambda, T_{i-1}(x)) \right\rangle_{H_i} \right)^2} + \epsilon_i \\
&\leq \sup_{x\in X_i} \sqrt{\sum_{j=1}^{d_i} \left(\left\| f_j^{(i)*} \right\|_{H_i} \left\| k^{(i)}(\lambda, F^{(i-1)*}(x)) - k^{(i)}(\lambda, T_{i-1}(x)) \right\|_{H_i} \right)^2} + \epsilon_i \\
&= \sup_{x\in X_i} \left\| k^{(i)}(\lambda, F^{(i-1)*}(x)) - k^{(i)}(\lambda, T_{i-1}(x)) \right\|_{H_i} \sqrt{\sum_{j=1}^{d_i} \left\| f_j^{(i)*} \right\|_{H_i}^2} + \epsilon_i \\
&\leq \sup_{x\in X_i} \sqrt{\left(L^{(i)}_{F^{(i-1)*}(x)} + L^{(i)}_{T_{i-1}(x)} \right) \left\| F^{(i-1)*}(x) - T_{i-1}(x) \right\|_2} \sqrt{\sum_{j=1}^{d_i} \left\| f_j^{(i)*} \right\|_{H_i}^2} + \epsilon_i \\
&\leq \sqrt{2L^{(i)} \sum_{j=1}^{d_i} \left\| f_j^{(i)*} \right\|_{H_i}^2} \sqrt{\left\| F^{(i-1)*} - T_{i-1} \right\|_s} + \epsilon_i,
\end{aligned}
$$

which proves the lemma. □

Proof of Lemma B.1. Since Ω and $\mathcal{F}_2$ are both closed under negation, we have

$$\begin{aligned}
\hat{\mathcal{G}}_N(\mathcal{F}_2 \circ \mathcal{F}_1) &= \mathbf{E} \sup_{\boldsymbol{\alpha}, F} \left| \frac{2}{N} \sum_{n=1}^{N} \sum_{\nu=1}^{m} \alpha_\nu k(F(x_\nu), F(x_n)) g_n \right| \\
&\leq \mathbf{E} \sup_{\boldsymbol{\alpha}, F} \frac{2}{N} \sum_{\nu=1}^{m} |\alpha_\nu| \sum_{n=1}^{N} k(F(x_\nu), F(x_n)) g_n \\
&\leq \frac{2}{N} A \mathbf{E} \sup_{F} \max_{\nu} \sum_{n=1}^{N} k(F(x_\nu), F(x_n)) g_n \\
&= \frac{2}{N} A \mathbf{E} \sup_{F} \max_{\nu} \sum_{n=1}^{N} \Big(k(F(x_\nu), F(x_n)) - k(F(x_\nu), 0) \Big) g_n \\
&\quad + \frac{2}{N} A \mathbf{E} \sup_{F} \max_{\nu} \sum_{n=1}^{N} k(F(x_\nu), 0) g_n \\
&\leq \frac{2}{N} A \mathbf{E} \sup_{F} \max_{\nu} \sum_{n=1}^{N} L_{F(x_\nu)} \|F(x_n)\|_2 g_n \\
&\leq \frac{2}{N} A L \mathbf{E} \sup_{F} \sum_{n=1}^{N} \|F(x_n)\|_2 g_n \\
&\leq \frac{2}{N} A L \mathbf{E} \sup_{F} \sum_{n=1}^{N} \|F(x_n)\|_1 g_n \\
&\leq A L d_1 \hat{\mathcal{G}}_N(\Omega).
\end{aligned}$$

Taking expectation with respect to the x_n finishes the proof. □

Proof of Lemma B.3. For $i \geq 1$, given the assumption that $d_{i-1} = d_i$, we first show that one can find an initialization for layer i, denoted $F^{(i)\circ}$, such that $F^{(i)\circ}(S) = F^{(i-1)}(S)$.

Without loss of generality, assume $i = 1$, then it amounts to showing that a set of parameters can be found for the kernel machines $f_1^{(1)}, \ldots, f_{d_1}^{(1)}$ of $F^{(1)}$ such that when these kernel machines are initialized with this certain set of parameters, this layer agrees with the identity function when restricted to S. Recall that $f_j^{(i)}(x) = \sum_{n=1}^{N} \alpha_{jn}^{(i)} k^{(i)}(x_n, x)$ and $\{\alpha_{jn}^{(i)} \in \mathbb{R} \mid n = 1, 2, \ldots, N\}$ is the set of trainable parameters for this kernel machine.

Solve equation $AG = D$ for A, where A is the $d_0 \times N$ matrix of parameters defined as $(A)_{nm} = \alpha_{nm}^{(1)}$, G is the $N \times N$ kernel matrix defined as $(G)_{nm} = k^{(1)}(x_n, x_m)$, D is a $d_0 \times N$ matrix whose n^{th} column is the nth example $x_n = (x_{n1}, x_{n2}, \ldots, x_{nd_0})^\top$ for $n = 1, 2, \ldots, N$. It is straightforward that the set of parameters A initializes $F^{(1)}$ to the desired $F^{(1)\circ}$. Moreover, A can always be solved in closed-form by inverting G since $k^{(1)}$ being PD guarantees that G is invertible.

Combining the above result and the defining property of gradient of the loss function with respect to the parameters, i.e., that gradient points at the direction of the greatest rate of increase of the loss function, we then have

$$\ell(F^{(0)}) = \ell(F^{(1)\circ}) \geq \ell(F^{(1)*}).$$

□

Proof of Lemma B.4. In this proof we shall again drop the layer index l for brevity.

Identify $f \in \mathcal{F}_A$ using w, b upto $\mathbb{R}$-scalar multiplication. Fix an F such that $\phi(F(S))$ is linearly separable (otherwise the learning paradigm is not applicable).

Let x_+, x_- be the closest pair of examples from distinct classes in H. For a given $f = (w, b)$, let x_-^w, x_+^w be a pair of examples from different classes that are closest to f in H in the sense that $f(F(x_+^w)), f(F(x_-^w))$ are the smallest in absolute value among all x_+, x_-, respectively. Denote the

canonical form of f with respect to $\phi(F(S))$ with equality attained by at least one of x_+^w, x_-^w as $f_F = (w_F, b_F)$, i.e., f_F satisfies $y f_F(x) \geq 1$ for all examples in $(x_n, y_n)_{n=1}^N$ and for at least one of x_-^w, x_+^w, the equality is attained. Define $A_{f_F} \coloneqq \inf_{b_F \in \mathbb{R}} \|w_F\|_H$.

Suppose the algorithm returns $f^\star = (w^\star, b^\star)$ and recall that A is the smallest such that $f^\star \in \mathcal{F}_A$, then for all $f = (w, b) \in \mathcal{F}_A$ such that $\hat{R}(f) = 0$,

$$A \geq \|w\|_H \geq \|w_F\|_H \geq A_{f_F}.$$

And it is easy to see that the last equality holds if and only if b_F is such that $y_-^w f_F(x_-^w) = y_+^w f_F(x_+^w)$. Then $f_F \in \mathcal{F}_A$. Since $\hat{R}(f_F) = 0$ and we have the freedom to choose b_F such that the last equality holds, by construction of the learning paradigm and the minimality of A, we have

$$A = \min_{\substack{f \in \mathcal{F}_A \\ \hat{R}(f)=0}} A_{f_F} = A_{f_F^\star}.$$

In canonical form, for any $f_F \in \mathcal{F}_A$, choose b_F such that $\|w_F\|_H = A_{f_F}$, then

$$\begin{aligned}
\frac{2}{A_{f_F}} &= \frac{1}{A_{f_F}} \big\langle \phi(F(x_+^w)) - \phi(F(x_-^w)), w_F \big\rangle_H \\
&\leq \frac{1}{A_{f_F}} \big\langle \phi(F(x_+)) - \phi(F(x_-)), w_F \big\rangle_H = \big\|\phi(F(x_+)) - \phi(F(x_-))\big\|_H \cos\theta_{F,w}.
\end{aligned}$$

By construction of the learning paradigm, $f^\star$ must make the equality hold and satisfy $\theta_{F,w^\star} = 0$. Hence we have

$$A = A_{f_F^\star} = \frac{2}{\big\|\phi(F(x_+)) - \phi(F(x_-))\big\|_H},$$

which proves that, as a function of F, A achieves its minimum if and only if F maximizes $\big\|\phi(F(x_+)) - \phi(F(x_-))\big\|_H$. Since

$$\begin{aligned}
&\arg\max_F \big\|\phi(F(x_+)) - \phi(F(x_-))\big\|_H \\
&= \arg\max_F \Big(\big\|\phi(F(x_+))\big\|_H^2 + \big\|\phi(F(x_-))\big\|_H^2 - 2\big\langle \phi(F(x_+)), \phi(F(x_-)) \big\rangle_H \Big) \\
&= \arg\min_F k\big(F(x_+), F(x_-)\big),
\end{aligned}$$

where we have used the assumption on k, namely, that $k(x, x) = \langle \phi(x), \phi(x) \rangle_H = \|\phi(x)\|_H^2 = c$, for all x. It immediately follows that any minimizer F of A must minimize $k(F(x_+), F(x_-))$ for all pairs of examples from opposite classes. This proves the desired result. □